



Supplement of

Radiative forcing bias of simulated surface albedo modifications linked to forest cover changes at northern latitudes

R. M. Bright et al.

Correspondence to: R. M. Bright (rbr@skogoglandskap.no)

S1. Contents

This supporting material file is structured as follows:

- **S2. Additional Material and Methods**
- **S3. Description of Albedo Parameterizations in Land Surface Models (Schemes)**
- **S4. Regression Model and Theoretical Basis**
- **S5. Daily Albedo Time Series: Observations vs. Predictions**
- **S6. Contribution Analysis: Snow Metamorphosis and Vegetation Structure**

S2. Materials and Methods

S.2.1. Regional geography and climate

The forests in our study region may be considered part of the boreal forest that extends as an almost continuous belt around the upper northern hemisphere. Managed forests of the region (Fig. 1) are dominated by Norway spruce (*Picea abies* H. Karst.), Scots pine (*Pinus sylvestris* L.) and Birch (*Betula pendula* Roth and *B. pubescens* Ehrh.), with understory vegetation often dominated by bilberries (*Vaccinium myrtillus* L.), other *Vaccinium* species, and various herb communities (Granhus et al., 2012). The region experiences a continental climate ('Subarctic/Boreal') characterized by long cold winters with short mild summers and moderate, seasonally distributed precipitation (Peel et al., 2007). Where logging activities are concentrated, snow covers the ground from December through early April in the lower elevations of the central, southern, and eastern parts of the region (ca. 200 m) – and from late October through early May in the northern and western parts of the region (ca. 800 m) (Norwegian Meteorological Institute, 2013b)

S.2.2. 2007-2009 Nov. – May daily historical meteorology

Daily historical meteorological time series for our three case regions are presented in Figure S2. Note that Nov. and Dec. 2006 are excluded.

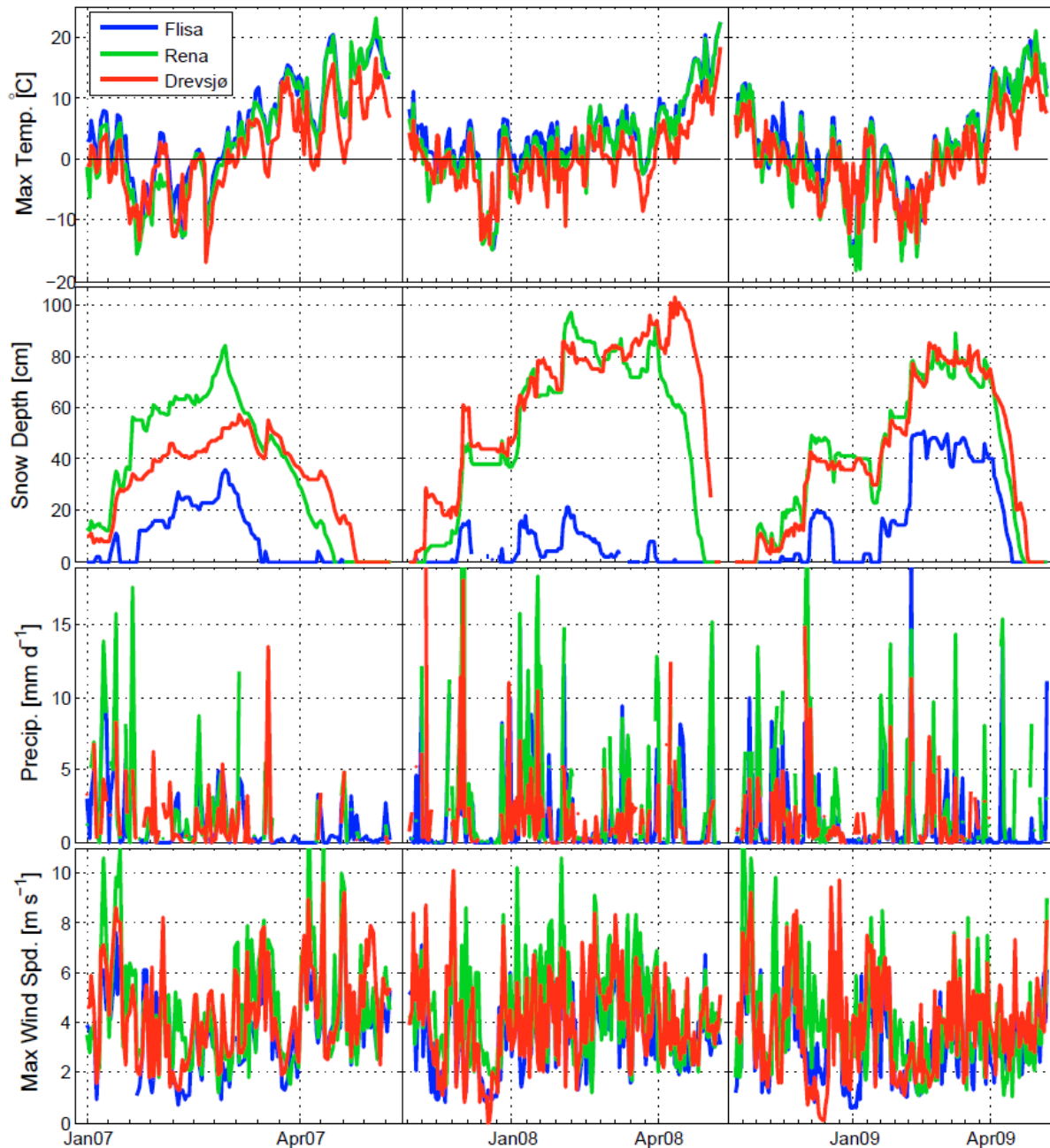


Figure S1. 2007 – 2009 observed daily meteorology [10 m], Nov. – May (excludes Nov. & Dec. 2006).

S.2.3. 2007-2009 daily albedo over forests, Nov. – May

Daily MODIS “black-sky” albedo (MCD43A) in evergreen needleleaf forests in each of our study regions. Note that Nov. and Dec. 2006 are excluded.

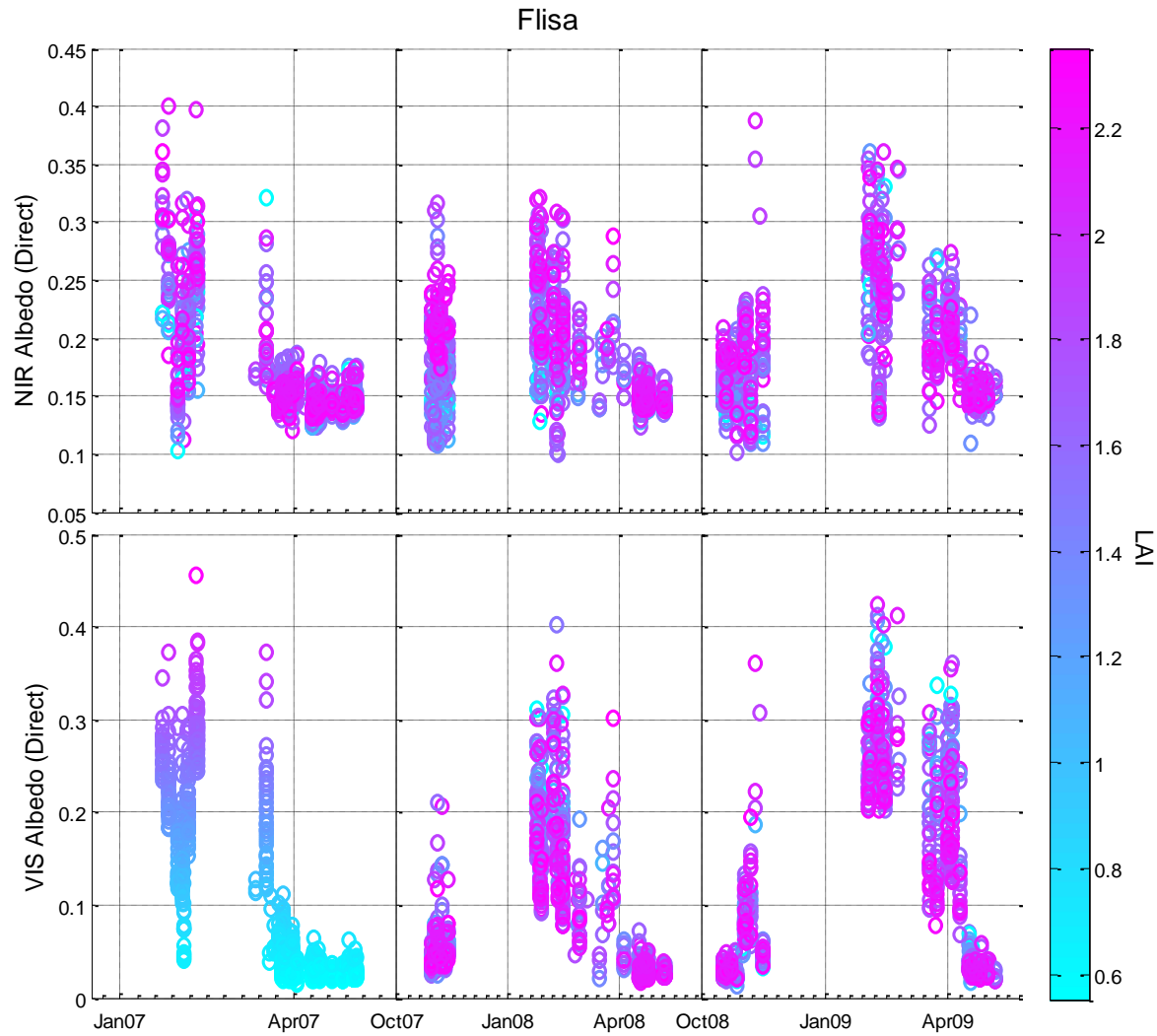


Figure S2. MODIS direct beam (“black sky”) daily albedo time series for the study region in Flisa municipality, Hedmark, Norway.

Large snow events in the coldest months of Jan. and Feb. in Flisa combined with high snow interception rates by forested canopies enhanced canopy albedo, resulting in higher albedos in forests with high LAIs (Figure S3).

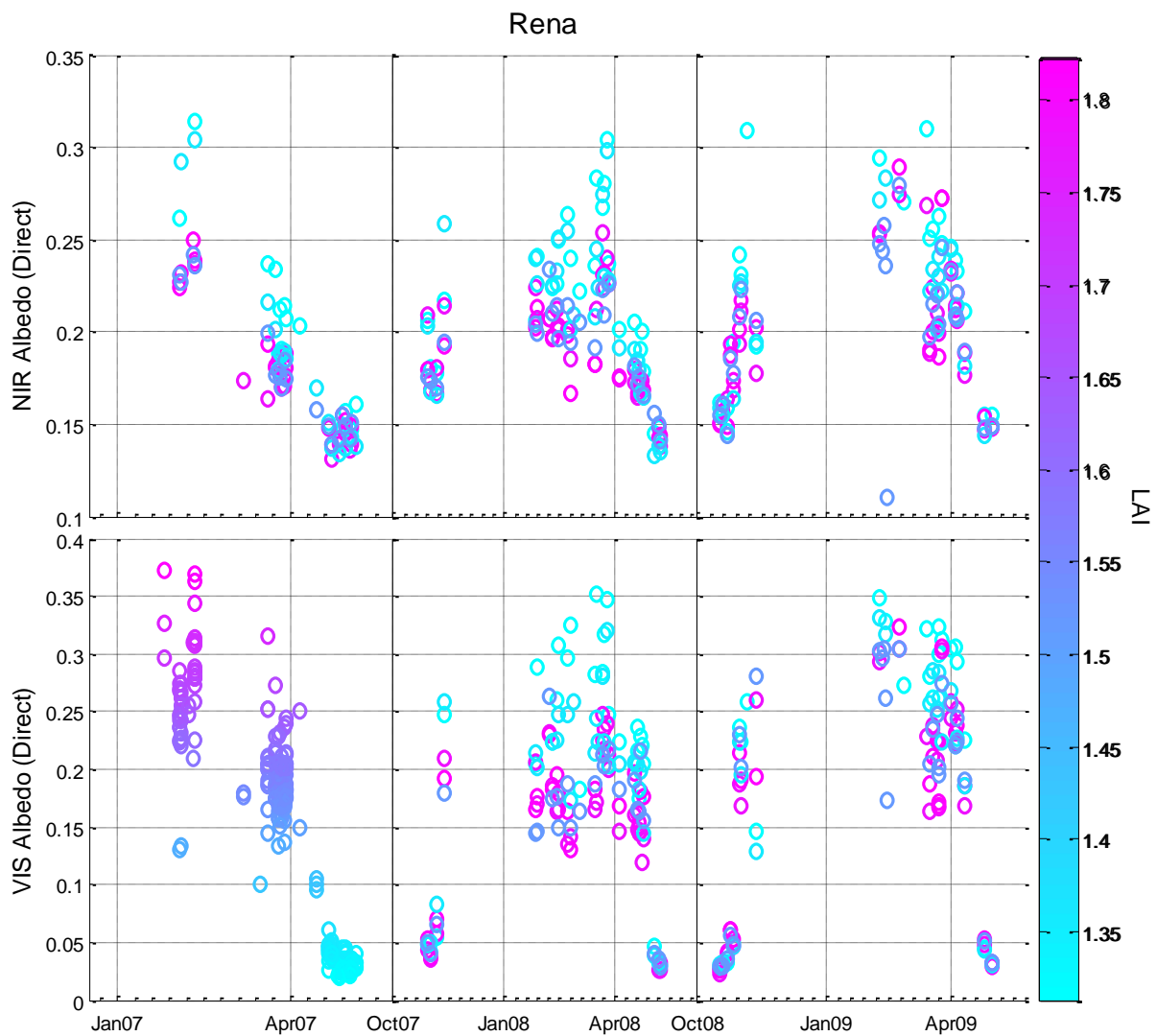


Figure S3. MODIS direct beam (“black sky”) daily albedo time series for the study region in Rena municipality, Hedmark, Norway.

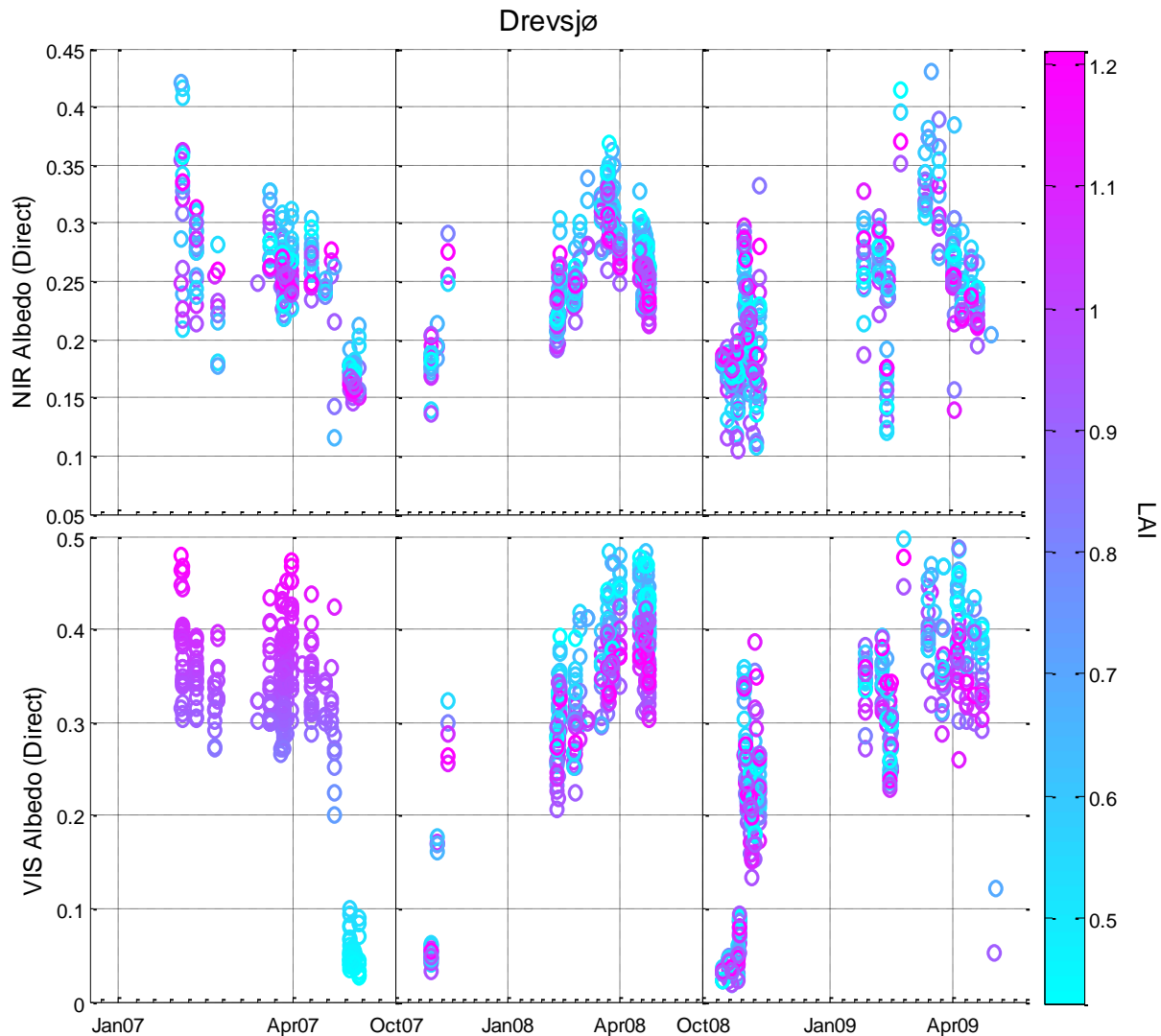


Figure S4. MODIS direct beam (“black sky”) daily albedo time series for the study region in Drevsjø municipality, Hedmark, Norway.

S.3. Albedo parameterizations in Land Surface Models (or schemes)

The following sub-sections contain descriptions of the albedo schemes in the land models included in our study. We do not comprehensively review and describe albedo parameterizations in land models or snow physical models, as this has been done extensively in recent years. See refs. (Essery et al., 2013; Mölders et al., 2008; Pedersen and Winther, 2005; Pirazzini, 2009; Rutter et al., 2009; Wang and Zeng, 2009).

S.3.1. JULES (2-stream)

The Joint UK Land-Environment Simulator (JULES) employs a two-stream approximation of radiation interception adopted from Sellers (Sellers, 1985) to calculate surface spectral albedos (Best et al., 2011; Essery et al., 2001). Optical parameter values and all parameterizations used in this study stem from the JULES technical documentation (Best, 2009).

Snow albedos are calculated using a simplified parameterization of a spectral snow albedo model (Wiscombe and Warren, 1980) in which snow aging is based on prognostic grain size, with minimum and maximum values set to 50 μm and 2000 μm , respectively. Fresh snowfall rates of 2.5 mm d⁻¹ (kg m³) reset grain size to its minimum, and grain area growth rate is determined by surface temperature, distinguishing between fresh and aged cold snow at grain size thresholds of 150 μm .

Canopy-intercepted snow is not parameterized in the JULES 2-stream model version applied in this study (Best, 2009); thus, surface albedo is parameterized as the weighted fraction of the zenith angle dependent direct beam snow albedo α_s and snow-free albedo α_0 as determined by snow cover fraction:

$$\alpha = f_s \alpha_s + (1 - f_s) \alpha_0 \quad (\text{S1})$$

where snow cover fraction f_s is parameterized following Oleson (2004) and is based on snow depth d and momentum roughness length z_0 :

$$f_s = \frac{d}{d + 10z_0} \quad (\text{S2})$$

Momentum roughness length z_0 is based on vegetation height h , where for “trees”, z_0 is set to $h/20$. In our simulations, h is based on airborne LIDAR measurements (H80). Height statistics per region are shown in Table S1.

S.3.2. JULES (All-band)

The snow albedo scheme in the “All-band” version of JULES is diagnostic, where snow albedo α_s takes the albedo of cold deep snow α_{cds} for temperatures below -2 C and a value between the snow-free albedo α_0 and α_{cds} when temperatures are between -2 C and the melting point of snow. Snow-free and cold deep snow albedos are estimated using a parameterization for radiative fraction f_r that is based on the 1-sided leaf area index (LAI):

$$\alpha_0 = (1 - f_r) \alpha_{soil} + f_r \alpha_s^\infty \quad (\text{S3})$$

$$\alpha_{cds} = (1 - f_r) \alpha_s^0 + f_r \alpha_s^\infty \quad (\text{S4})$$

where α_{soil} is the albedo of snow-free soil underlying vegetation and α_s^0 , α_0^∞ , and α_s^∞ are the vegetation-dependent albedos. Albedo parameters of the “All-band” version are presented in Best et al. [2009]. However, since our radiative transfer model differentiates between NIR and VIS bands, we instead take observed latitude- and vegetation-dependent NIR and VIS albedos for “Grassland” and “Needleleaf Forests reported in Gao et al (2005) and observed soil albedos from Lawrence & Chase (2007), shown in Table S2. Maximum values for vegetation-dependent cold deep snow albedos are used (α_s^0) and Eq. S4 is ignored since band-dependent α_s^∞ values are unavailable.

Table S1. Vegetation-dependent snow-free albedos are means for IGBP Class “Evergreen Needleleaf” (60-70° N) and “Grasslands” (50-70° N), while vegetation-dependent snow albedos are maximums (α_s^0) (Gao et al., 2005). Soil albedos values are means of dry and saturated values reported in Table 4 of Lawrence & Chase (2007).

	NIR	VIS
α_{soil}	0.170	0.090
α_0^∞ , “Evergreen Needleleaf”	0.160	0.024
α_0^∞ , “Grassland”	0.241	0.063
α_s^0 , “Evergreen Needleleaf”	0.222	0.279
α_s^0 , “Grassland”	0.569	0.831

Total surface albedo α is parameterized as a combination of the snow-free albedo α_0 and a weighted value based on snow mass:

$$\alpha = \alpha_0 + (\alpha_s - \alpha_0)(1 - e^{-0.2S}) \quad (S5)$$

Where S is snow mass (kg m^{-2}) and α_s and α_0 are the snow and snow-free albedo, respectively. We estimate S using observed snow depth (Norwegian Meteorological Institute, 2013a) and an empirical model of snow density based on meteorological predictors (Meløysund et al., 2007).

S.3.3. CLM4

Direct beam albedos in the Community Land Model version 4.0 (CLM4) are calculated from the two-stream approximation of Dickinson (1983) and Sellers (1985) assuming a random distribution of leaf angles and using mean canopy LAI observations (based on airborne LIDAR) and a SAI of 1 from Zeng et al. (2002). All vegetation and intercepted snow optical parameters are taken from the CLM4.0 technical documentation (2010) which are based on the works of Dorman & Sellers (1989) and Asner (1998). Spectral-dependant soil albedos are the mean “Boreal” wet and dry values presented in Lawrence & Chase (2007) which are based on MODIS observations.

Canopy snow fraction f_{cs} is determined by intercepted snow which is based on accumulated snow loading and unloading and a maximum interception capacity determined by total leaf and stem area index ($LSAI = LAI + SAI$) and an empirical constant from Dickinson et al. (1993). The albedo of the canopy is based on the exposed fraction $LSAI_{ex}$:

$$LSAI_{ex} = LSAI(1 - f_{cs}) \quad (S6)$$

In this study we do not employ the snow radiative transfer model SNICAR and thus do not account for snow impurities from aerosol deposition; instead, we rely on the same simplified parameterizations of the snow spectral models (Wiscombe and Warren, 1980) employed in JULES (Best, 2009). Snow aging is based on effective grain size evolution in a single snow layer that is prognosed by near-surface temperature as a proxy, since we do not employ the snow

physics model needed to obtain snow temperature, temperature gradients (multiple layers), or densities. The minimum effective grain radius of fresh snow is 54.5 μm and the maximum for refrozen liquid water is set at 1000 μm .

Ground albedo is a weighted share of soil and the zenith angle dependent snow albedo, where the parameterization for the fraction of ground covered by snow f_s is based on the work of Niu and Yang (2007):

$$f_s = \tanh\left(\frac{d}{2.5z_{0m,g}[\min(\rho_{snow}, 800) / \rho_{new}]^m}\right) \quad (\text{S7})$$

Where d is snowdepth (m), $z_{0m,g}$ is momentum roughness length of soil (0.01 m), ρ_{new} is the density of fresh snow set at 100 kg m^{-3} , ρ_{snow} is the snow density in the current time step, and m an empirical constant set at 1 for global applications. Since the snow physics model is needed to estimate ρ_{snow} , we rely instead on an empirical parameterization described in Meløysund et al. (2007) based on common meteorological predictors.

S.3.4. JSBACH

The albedo scheme in the Jena Scheme for Biosphere-Atmosphere Coupling in Hamburg (JSBACH) distinguishes between the albedo of snow on the ground and snow intercepted in forest canopies (Reick et al., 2012):

$$\alpha = f_g [(1 - f_s)\alpha_{g0} + f_s\alpha_{gs}] + (1 - f_g)[(1 - f_c)\alpha_{c0} + f_c\alpha_{cs}] \quad (\text{S8})$$

where f_g is the exposed ground (“canopy gap”) fraction, f_c fraction of canopy covered with snow, and f_s is the snow-covered ground fraction. Values for broadband NIR and VIS albedos for snow-covered canopies α_{sc} , snow-covered ground α_{sg} , exposed ground α_{g0} , and canopy α_{c0} are from Otto et al. (2011) .

Table S2. Albedo values applied in our analysis, from Otto et al. (2011) .

	NIR	VIS
α_{g0} ^a	0.28	0.05
α_{c0}	0.26	0.05
α_{sg} , max	0.7	0.9
α_{sg} , min	0.3	0.5
α_{sc}	0.25	0.25

^a “Shrubs cold” PFT

The fraction of exposed ground f_g is a function of leaf and stem (“plant”) area indices (LSAI):

$$f_g = e^{-LSAI} \quad (\text{S9})$$

where a value of 1 for SAI is used for all forest PFTs. The albedo of snow covered ground α_{sg} decreases linearly with surface temperature that ranges from a minimum value at melting point to a maximum value for temperatures of less than -5°C ; the albedo of snow-covered canopies α_{sc} is fixed. Solar-zenith angle dependency of snow albedo is not taken into account in the scheme.

Canopy intercepted snow in JSBACH is estimated with the simple prognostic snow interception modeling scheme outlined in Roesch et al. (2001), where the intercepted snow is based on snowfall rate, unloading rate due to temperature (melt/drip and slipping), unloading rate due to wind, and sublimation. Parameterizations determining unloading rates from temperature and wind are adapted from the empirical works of Nakai et al. (1994), Yamazaki et al. (1996), Betts & Ball (1997), and Miller (1962). Canopy intercepted snow is limited by a maximum storage capacity that is based on LAI (2 mm H₂O-eq./unit LAI), with the snow-covered fraction f_c as the ratio of intercepted snow to snow interception capacity.

Here, we exclude sublimation as we do not have the necessary meteorological data required to estimate vapor pressure gradients nor the capacity to model air exchange rates around the snow surface.

S.3.5. CLASS

Like JSBACH, the Canadian Land Surface Scheme (CLASS) distinguishes between snow intercepted in forest canopies and snow on ground (as in Eq. (S8)), and relies on plant area index (LSAI) to estimate the fraction of exposed ground (“sky-view”) in the same way (as Eq. (S9)) (Verseghy, 2009; Verseghy et al., 1993). However, the direct beam albedo may be calculated separately in CLASS and is zenith angle dependent for snow covered surfaces. Additionally, the albedo of ground underlying the forest canopy is weighted by canopy transmissivity – which is also zenith angle dependent – to account for the decreased shortwave radiation incident at ground surface.

Canopy transmissivity to shortwave radiation is obtained by applying a form of Beer’s law of radiation transfer in non-scattering media:

$$\tau_c = e^{-\kappa LSAI} \quad (\text{S10})$$

where the extinction coefficient κ is estimated following Goudriaan (1988) and is both PFT and spectral dependent

$$\kappa = \varepsilon O(\cos(SZA))^{-1} \quad (\text{S11})$$

where ε is a correction factor less than or equal to 1 accounting for forward scattering and non-random leaf distributions and O is the leaf distribution angle assumed to be 0.5 for randomly distributed leaves (needleleaf foliage). ε for needleleaf trees is 0.6 and 0.8, respectively, for NIR and VIS bands ($\varepsilon O = 0.3$ and 0.4).

In CLASS, canopy intercepted snow is parameterized following Hedstrom & Pomeroy (Hedstrom and Pomeroy, 1998) and is described by the balance between loading rate from fresh snowfall and unloading rate that is governed by an exponential empirical coefficient. Canopy

interception capacity is parameterized following Bartlett et al. (2006) and Schmidt & Gluns (1991) using plant area index (LSAI). The fraction of canopy covered in snow f_c is the ratio of intercepted snow to interception capacity.

CLASS employs a prognostic snow-albedo scheme that accounts for a declining albedo with snow age. In the absence of fresh snow, α_s decreases exponentially with time from its fresh value to an old value (Table S4, “old dry” snow) following Aguado (1985), Robinson & Kukla (1984), and Dirmhirn & Eaton (1975). If temperature is at or above freezing, a lower value for melting snow is applied (Table S4, “old melting” snow).

Table S3. Albedo values applied in our analysis, from Verseghy (2009).

	NIR	VIS
α_{g0}^a	0.19	0.03
α_{c0}	0.19	0.03
α_{sg} & α_{sc} , fresh	0.73	0.95
α_{sg} & α_{sc} , old dry	0.56	0.84
α_{sg} & α_{sc} , old melting	0.38	0.62

^a “Evergreen broadleaf shrub” PFT, Appendix Table A in Verseghy (2009).

Because it is not mentioned in Verseghy (2009), the albedo value for “fresh snow” is assumed to be reset if snowfall exceeds 2 mm d⁻¹ (H₂O-eq.).

S.3.6. GISS II

In the Goddard Institute for Space Studies (GISS) model II albedo scheme (Hansen et al., 1983) – which is still employed in the more recent “Model E” version (Schmidt et al., 2006) – total surface albedo α is parameterized in the same way as the JULES “All-band” scheme and is a combination of the snow-free albedo α_0 and a weighted value based on snow depth and surface masking depth. Snow albedo α_s is age-based and prognostic, where the albedo of fresh snow decays linearly as a function of time to a minimum value unless reset by 2 mm of fresh snowfall. The snow-free albedo α_0 and surface masking depth d_m terms are vegetation dependent, with those applied in this study shown in Table S5. Surface masking depth is 10 m.

Table S4. Albedo values are mean values for “Winter” and “Spring” in Hansen et al. (1983).

	NIR	VIS
α_0 , “Evergreen”	0.20	0.07
α_0 , “Grass”	0.31	0.10
α_s , fresh	0.6	0.90
α_s , old	0.35	0.60

S.4. Regression model

The best performing non-linear multiple regression model (in terms of Akaike's Information Criterion; ACC) is that which is based on a single predictor of forest structure and two climate predictors:

$$\alpha = \overbrace{k_1 + k_2(1 - e^{-LAI})}^{\text{Snow-free albedo}} + k_3 \tanh(d / k_4) \underbrace{\left(e^{-k_5(LAI)} + \left[1 - \frac{1}{1 + e^{-k_6 T^{MAX}}} \right] \right)}_{\text{w/Snow on ground & in canopy}} \quad (\text{S12})$$

Where d is snow depth (cm), T^{MAX} is the maximum daily temperature ($^{\circ}\text{C}$), and LAI is leaf area index ($\text{m}^2 \text{ m}^{-2}$). The forest canopy is distinguished from the ground surface with a sky-view factor e^{-LAI} (or canopy radiative fraction $(1 - e^{-LAI})$). The snow-free albedo in the absence of the forest canopy (i.e., the ground albedo) is represented by k_1 ; in the presence of the forest canopy, the snow-free albedo is the sum of k_1 and the term k_2 scaled by the canopy radiative fraction. In winter and spring, in addition to forest structure, meteorology plays a role in determining the total albedo. Those meteorological variables which have been found to significantly and consistently affect the albedo of snow-covered surfaces across a variety of sites and regions include temperature and snow depth (Broch et al., 2000; Mölders et al., 2008; Pedersen and Winther, 2005). Temperature plays a strong role in the metamorphosis of effective grain surface area (Aoki et al., 2003; Brun, 1989). Further, canopy unloading of intercepted snow due to slippage and melt, and thus the albedo of the forest canopy, is also greatly influenced by temperature (Kuusinen et al., 2012; Nakai et al., 1994; Yamazaki et al., 1996). Here, we find that maximum daily temperature (T^{MAX}) is a robust predictor of both the albedo of the forest canopy and snow-covered surface. The relationship with temperature can be described well with a logistic function, which is supported by analysis of others (Aoki et al., 2003; Bright et al., 2014; Bright et al., 2013).

Snow depth is often used in parameterizations of snow cover fraction (Niu and Yang, 2007; Roesch et al., 2001; Yang et al., 1997), with snow cover being important for the albedo of exposed ground. The relationship with the albedo of snow-covered ground and snow depth is best described with a hyperbolic tangent function which is in line with that originally proposed by Yang et al. (1997), later refined in Niu & Yang (2007), and currently used in the CLM4 scheme (Oleson et al., 2010). Here, the parameter k_4 replaces the snow density and roughness terms in refs. (Niu and Yang, 2007; Oleson et al., 2010) since these variables are not directly available.

Table S5. Regression model parameters and performance metrics. All parameters are statistically significant (p-values < 0.001).

Model	k_1	k_2	k_3	k_4	k_5	k_6	r^2	RMSE
SW (0.3 – 5 μm)	0.15	-0.06	0.27	4.58	2.69	0.05	0.86	0.045
NIR (0.7 – 5 μm)	0.19	-0.05	0.16	3.10	4.75	0.07	0.70	0.047
VIS (0.3 – 0.7 μm)	0.09	-0.07	0.37	4.55	2.01	0.04	0.89	0.058

We did not detect any strong correlation between albedo and solar zenith angle ($r = 0.21$), and further, we did not detect any strong negative correlation between wind speed and albedo ($r = -0.07$) from canopy unloading, as reported by others (Betts and Ball, 1997; Miller, 1962).

S.5. Daily Albedo Time Series: Observations vs. Predictions

S.5.1. JULES (All-band)

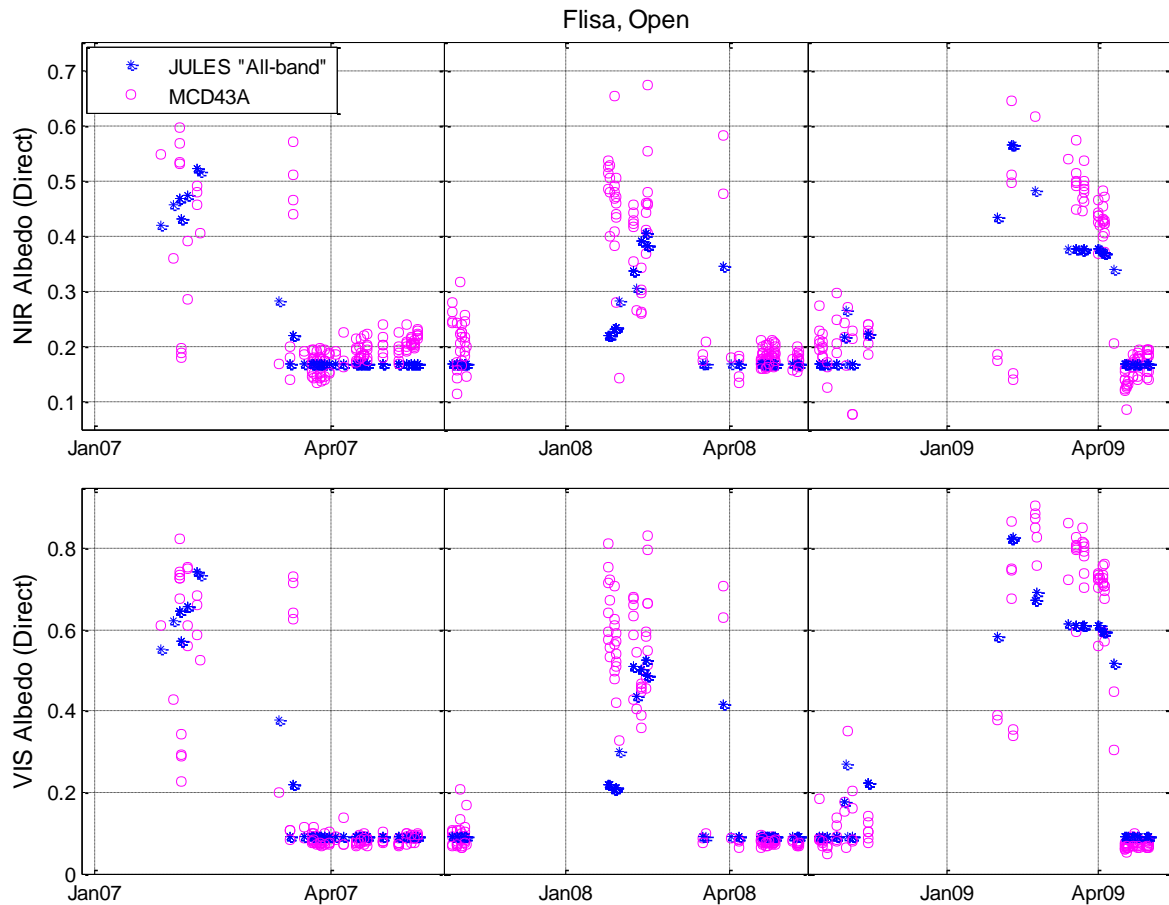


Figure S5. Predicted and observed daily black-sky albedo at the open sites (cropland) in Flisa.

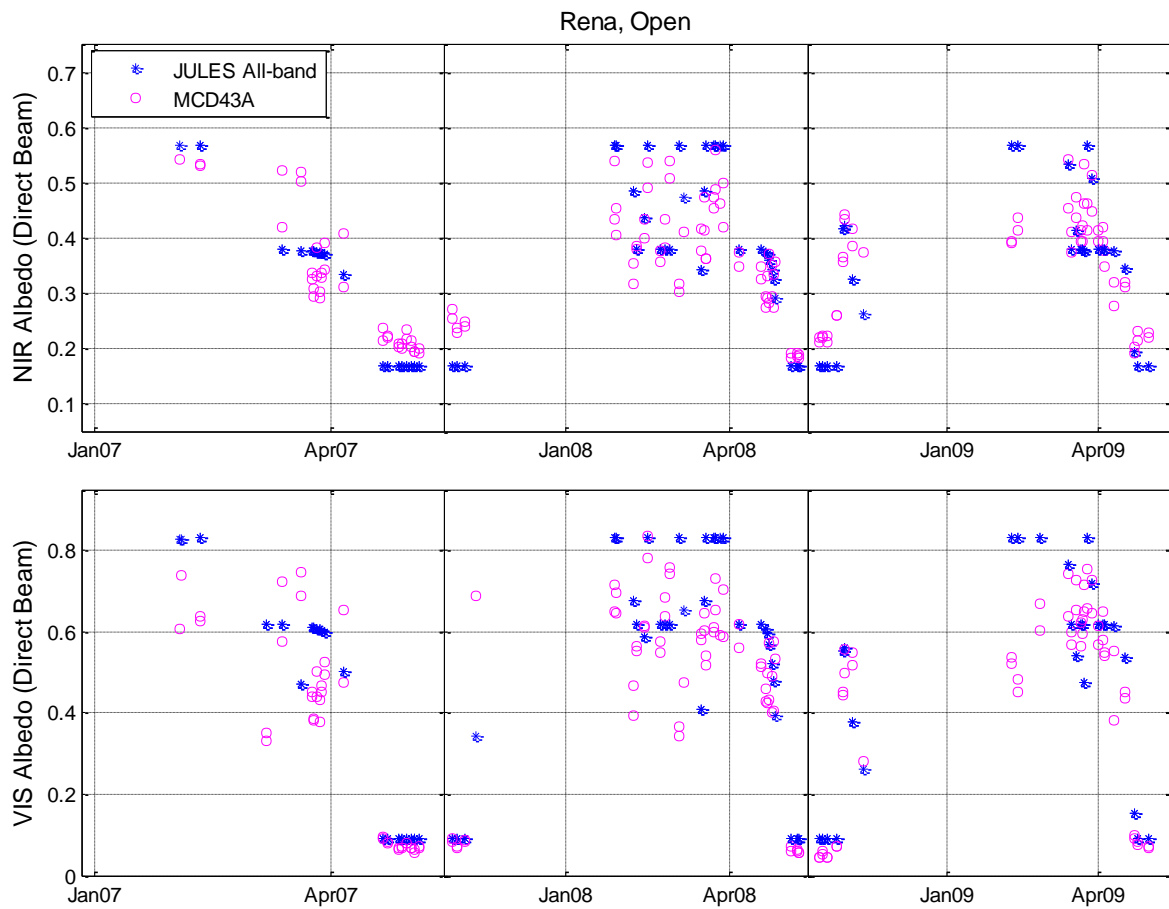


Figure S6. Predicted and observed daily black-sky albedo at the open sites (cropland) in Rena.

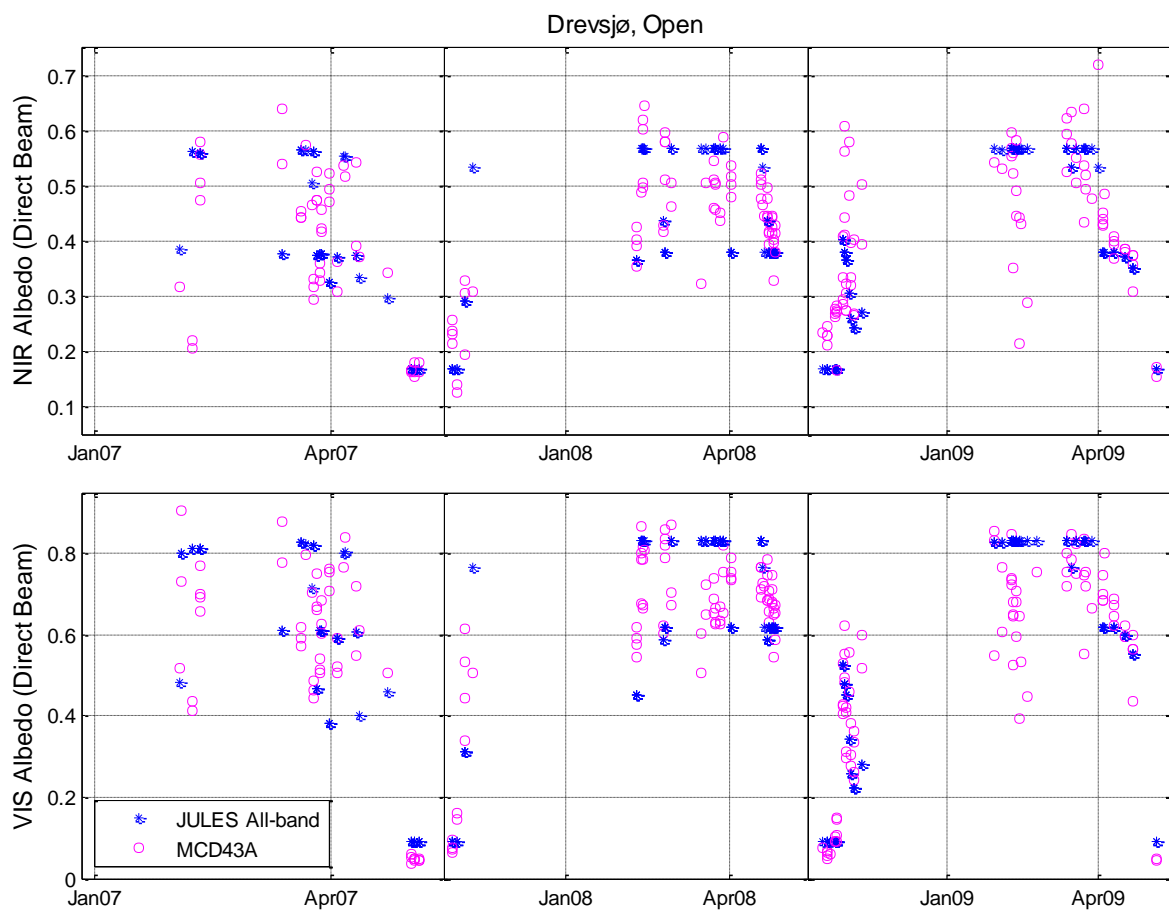


Figure S7. Predicted and observed daily black-sky albedo at the open sites (wetland/peatland) in Drevsjø.

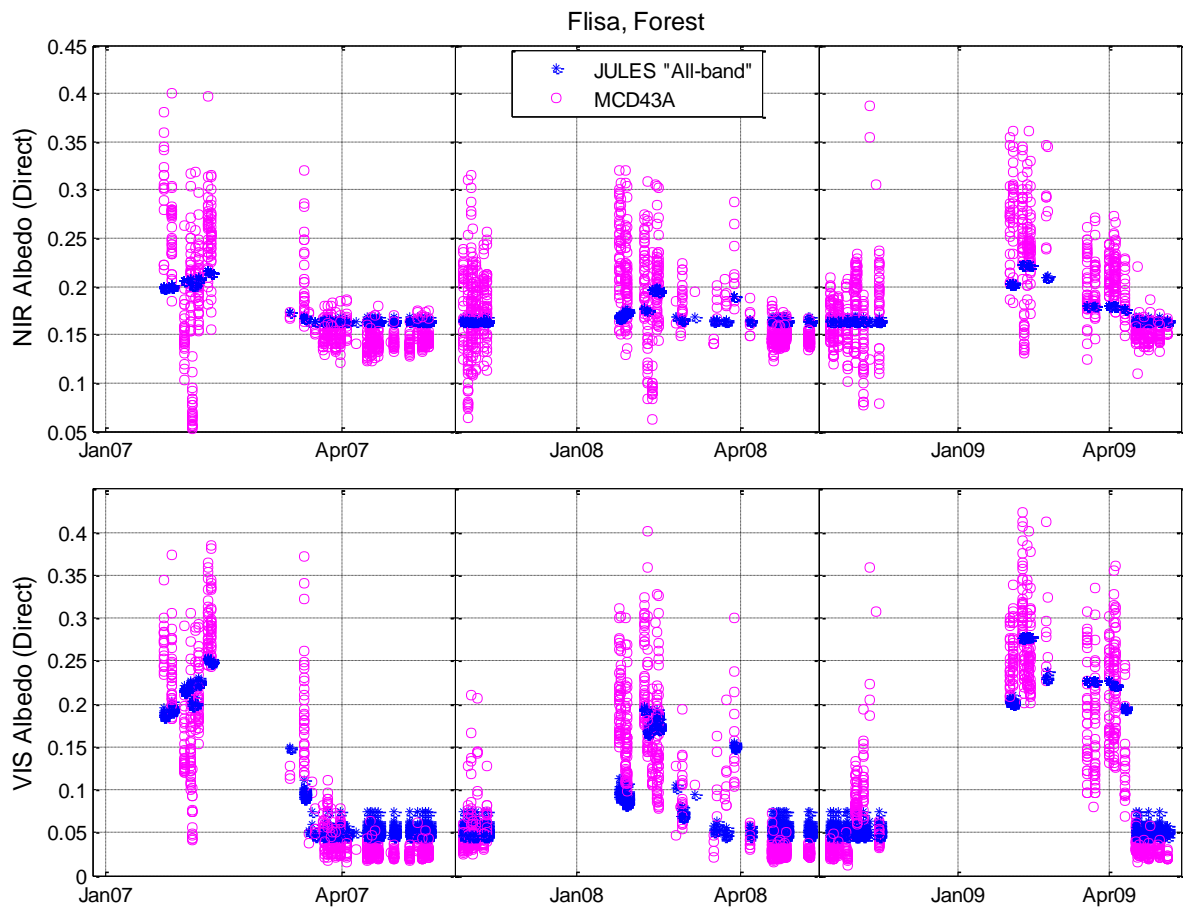


Figure S8. Predicted and observed daily black-sky albedo at the forested sites (evergreen needleleaf) in Flisa.

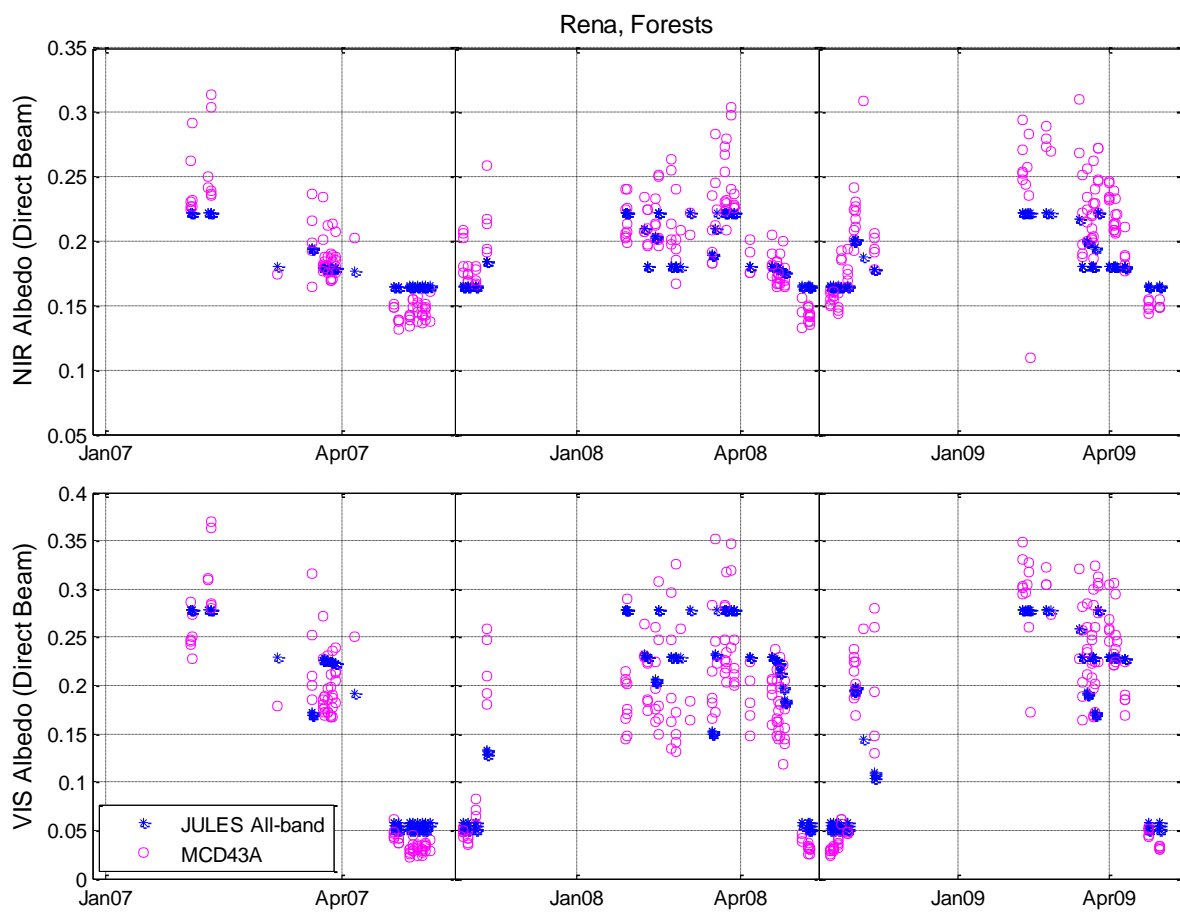


Figure S9. Predicted and observed daily black-sky albedo at the forested sites (evergreen needleleaf) in Rena.

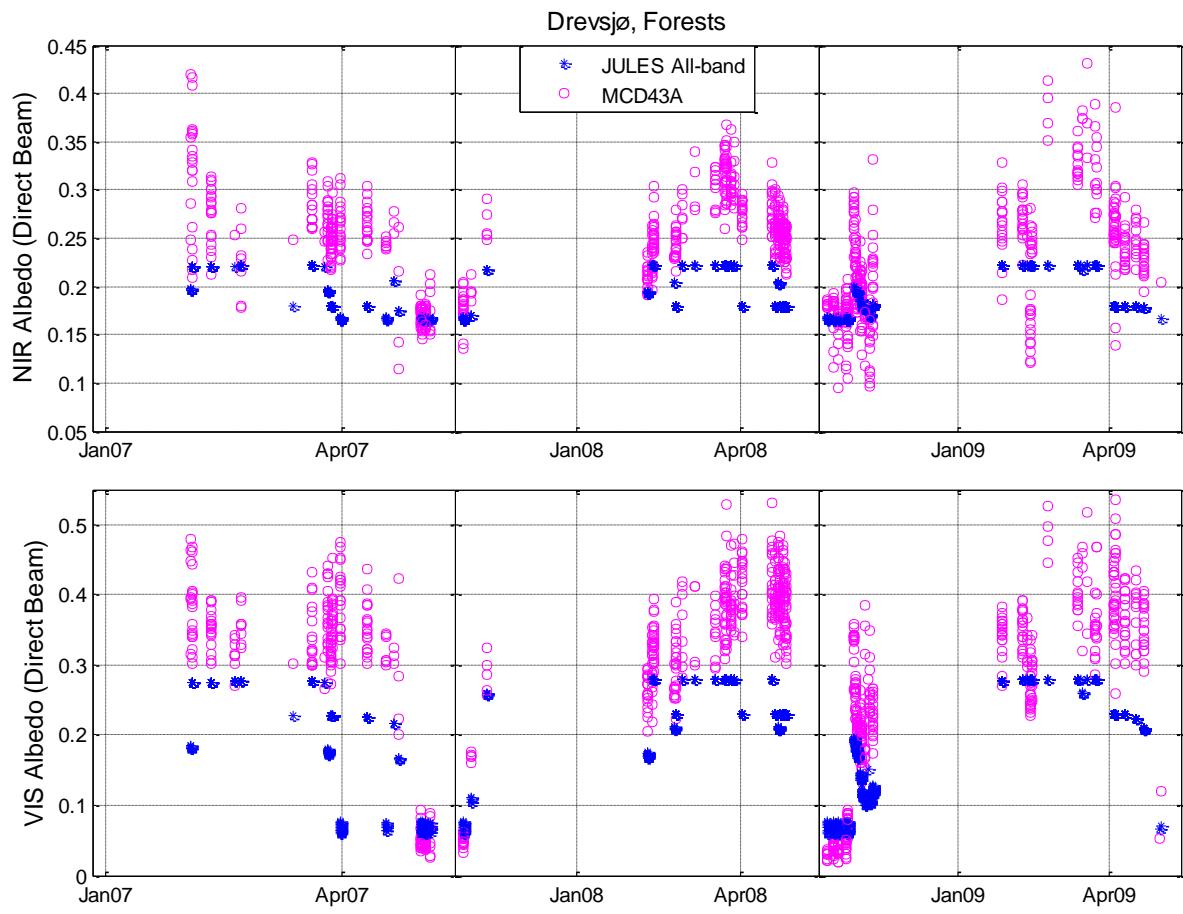


Figure S10. Predicted and observed daily black-sky albedo at the forested sites (evergreen needleleaf) in Drevsjø.

S.5.2. JULES 2-stream

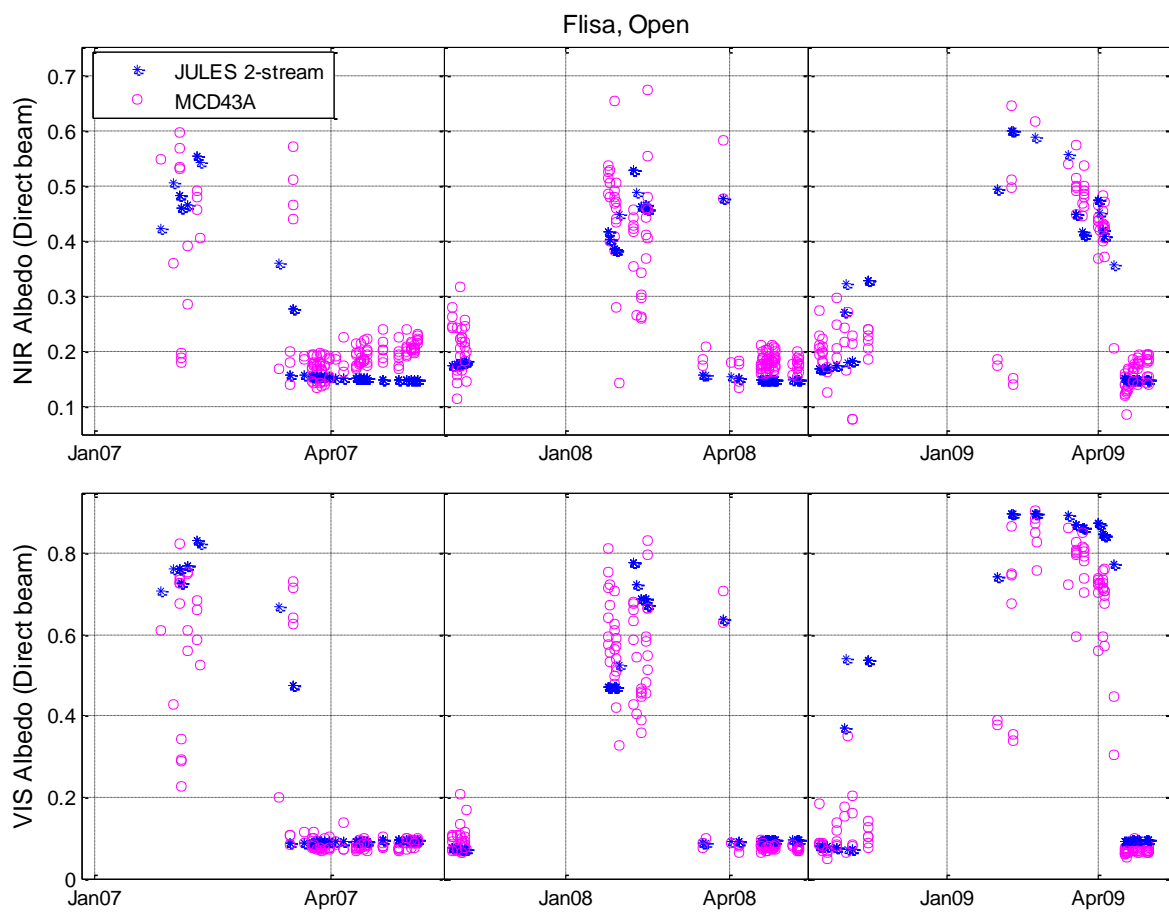


Figure S11. Predicted and observed daily black-sky albedo at the open sites (cropland) in Flisa.

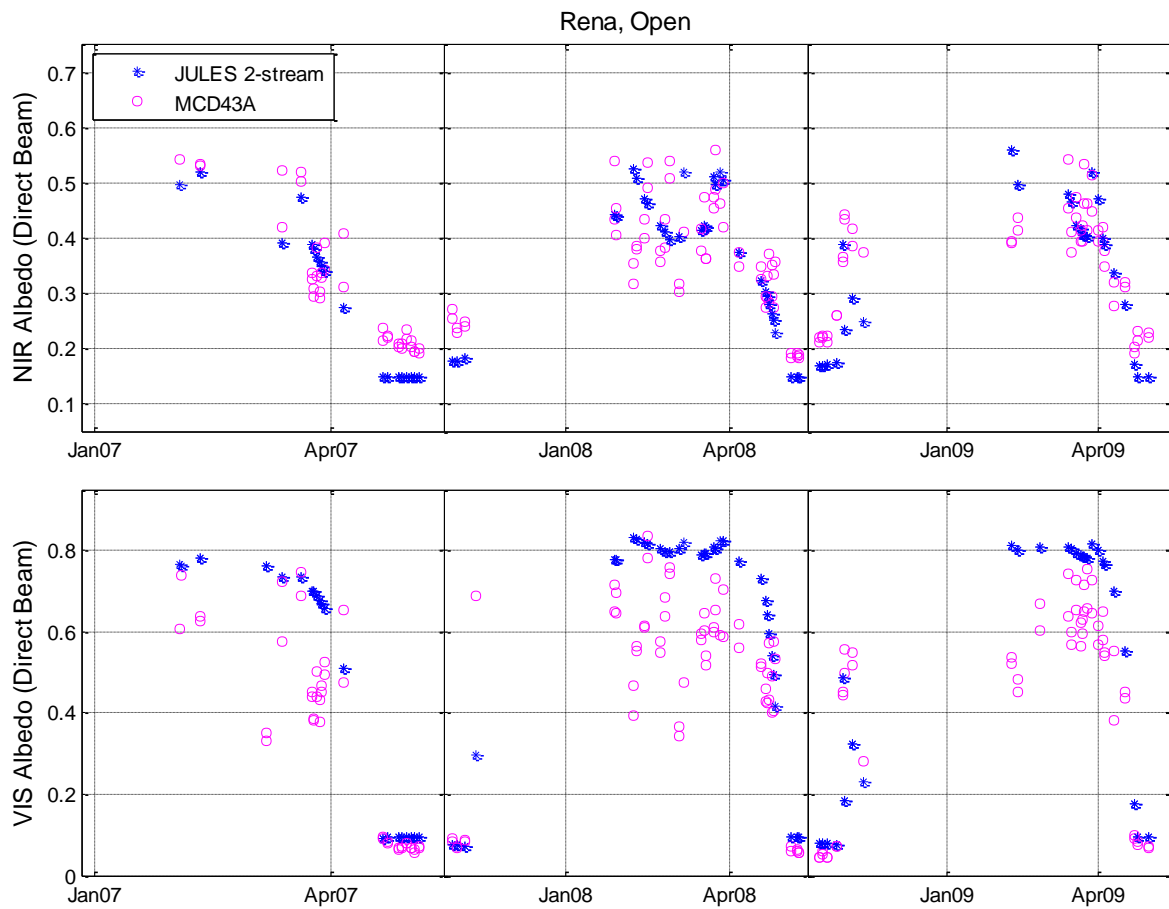


Figure S12. Predicted and observed daily black-sky albedo at the open sites (cropland) in Rena.

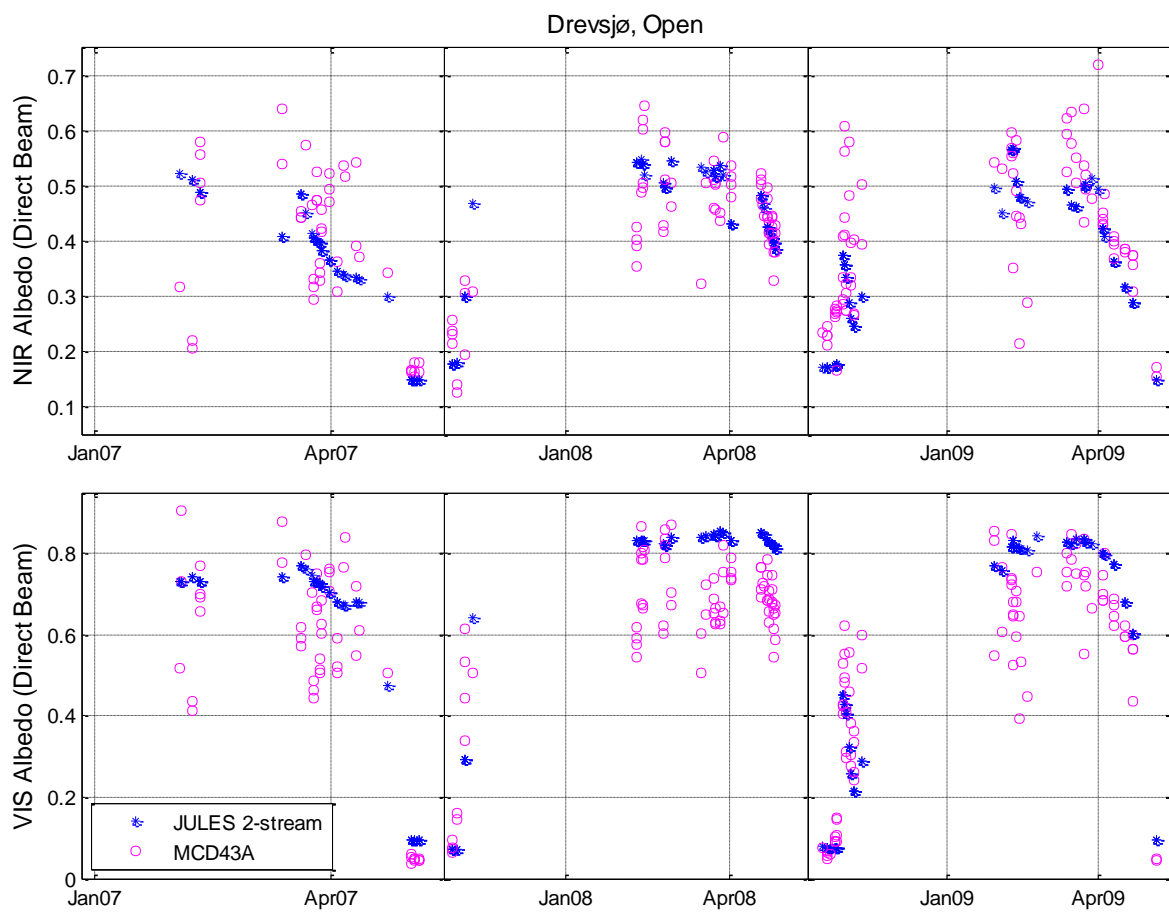


Figure S13. Predicted and observed daily black-sky albedo at the open sites (wetland/peatland) in Drevsjø.

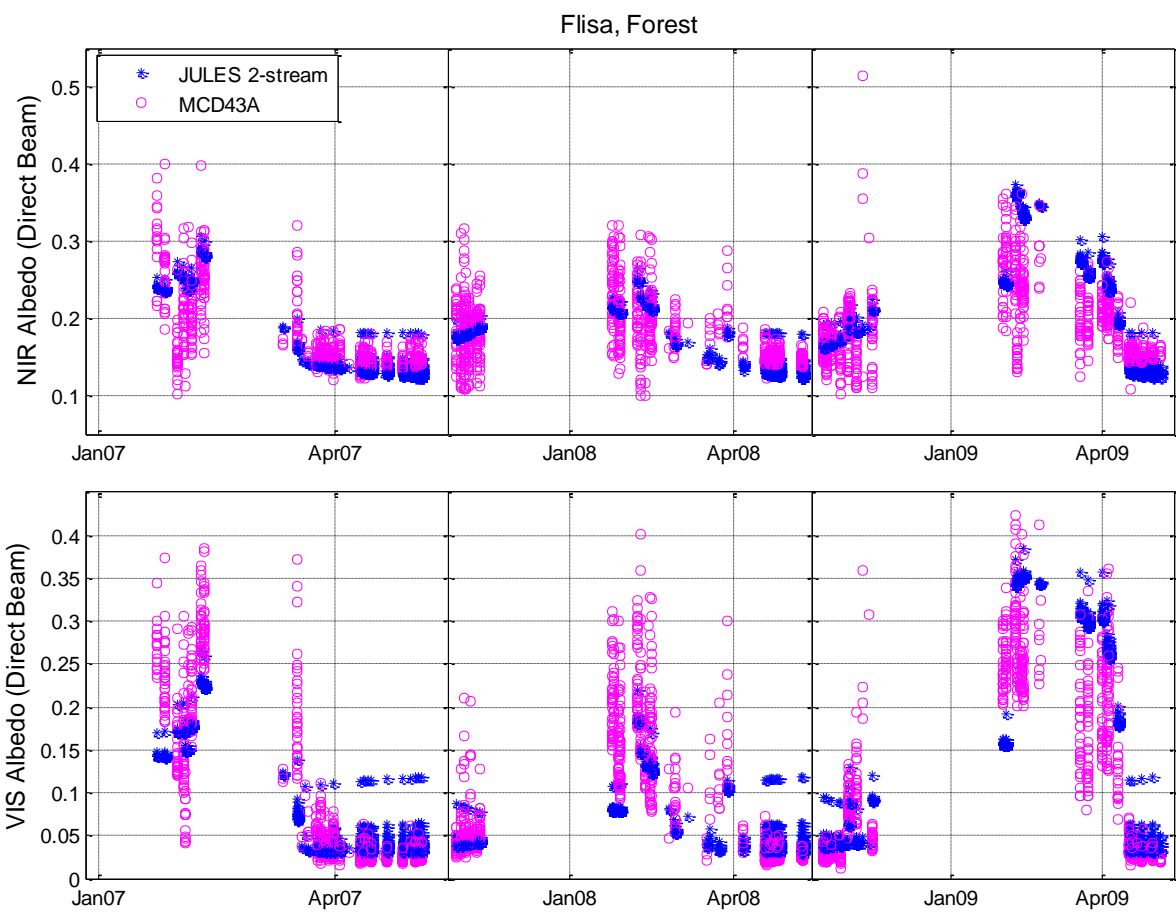


Figure S14. Predicted and observed daily black-sky albedo at the forested sites (evergreen needleleaf) in Flisa.

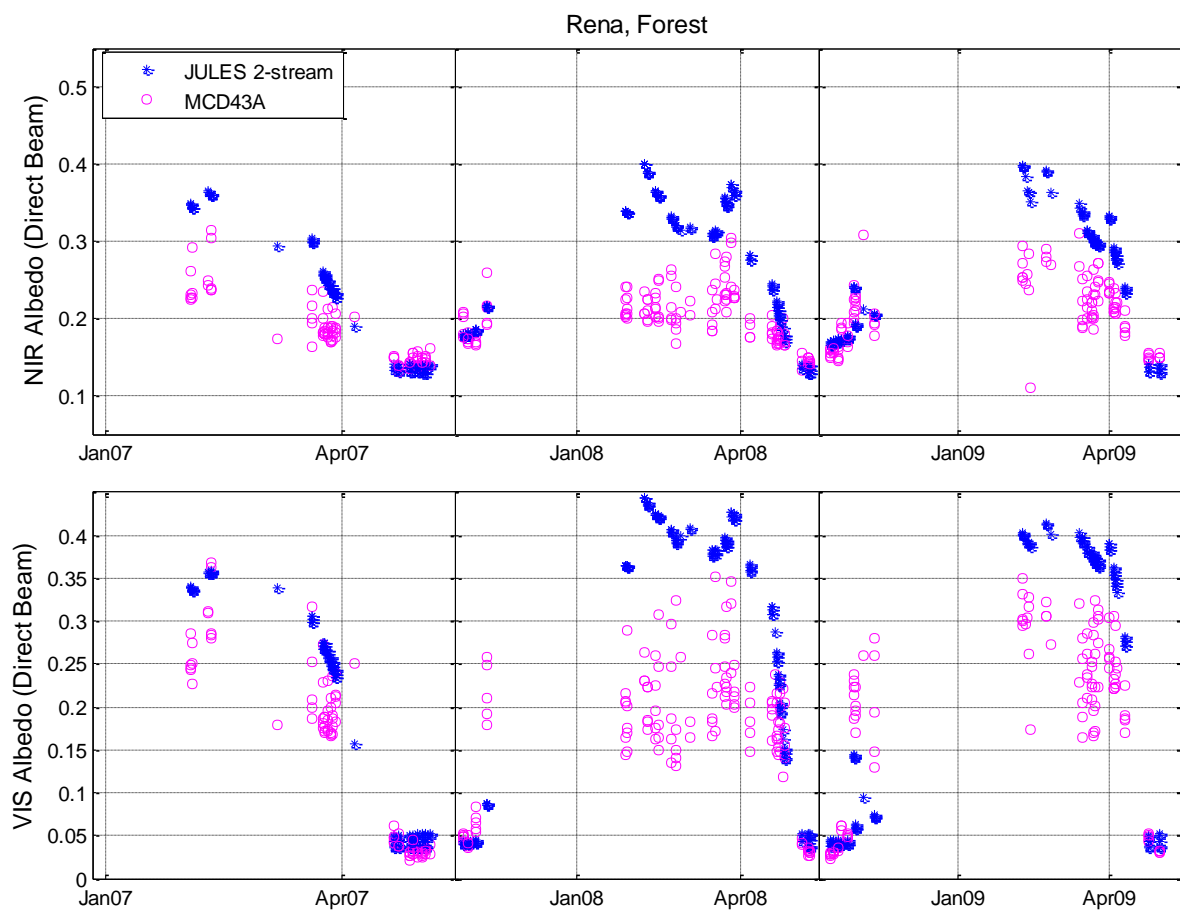


Figure S15. Predicted and observed daily black-sky albedo at the forested sites (evergreen needleleaf) in Rena.

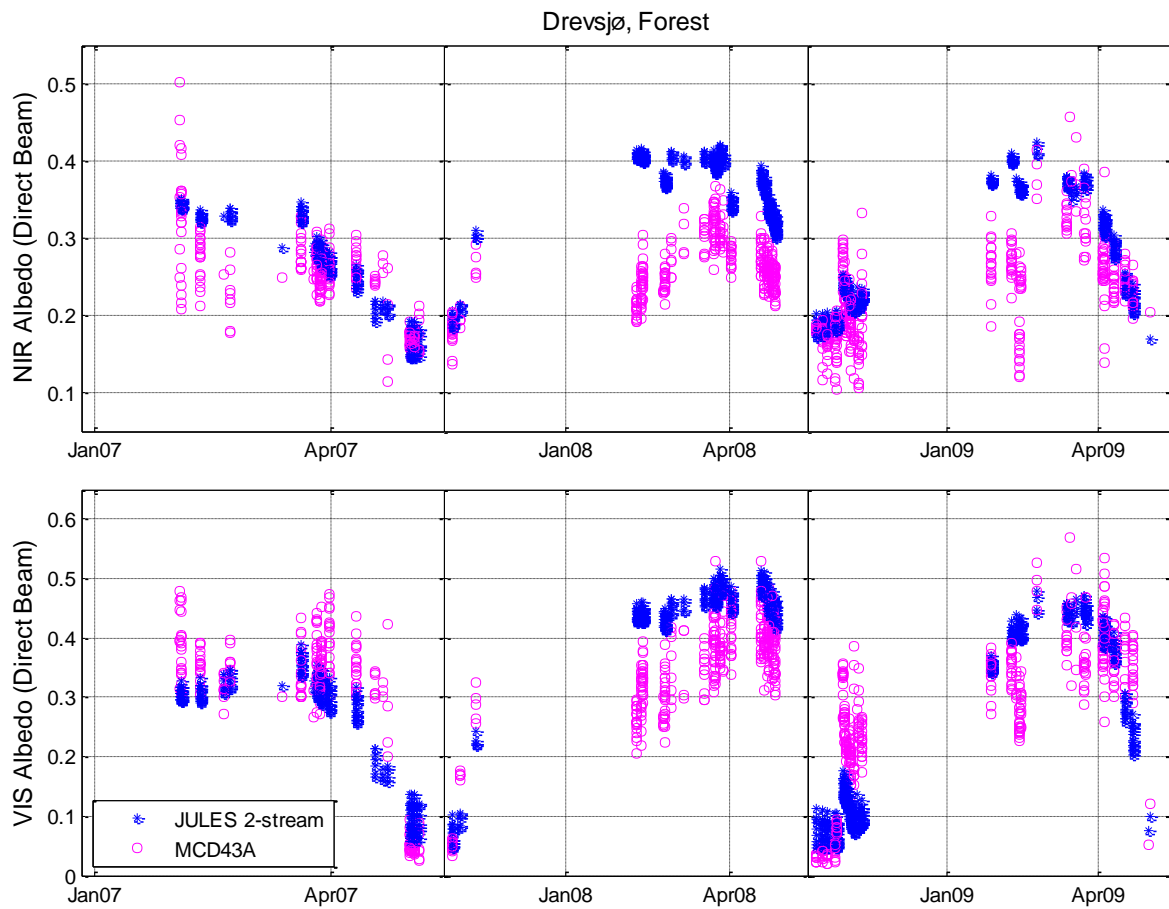


Figure S16. Predicted and observed daily black-sky albedo at the forested sites (evergreen needleleaf) in Drevsjø.

S.5.3. CLM4

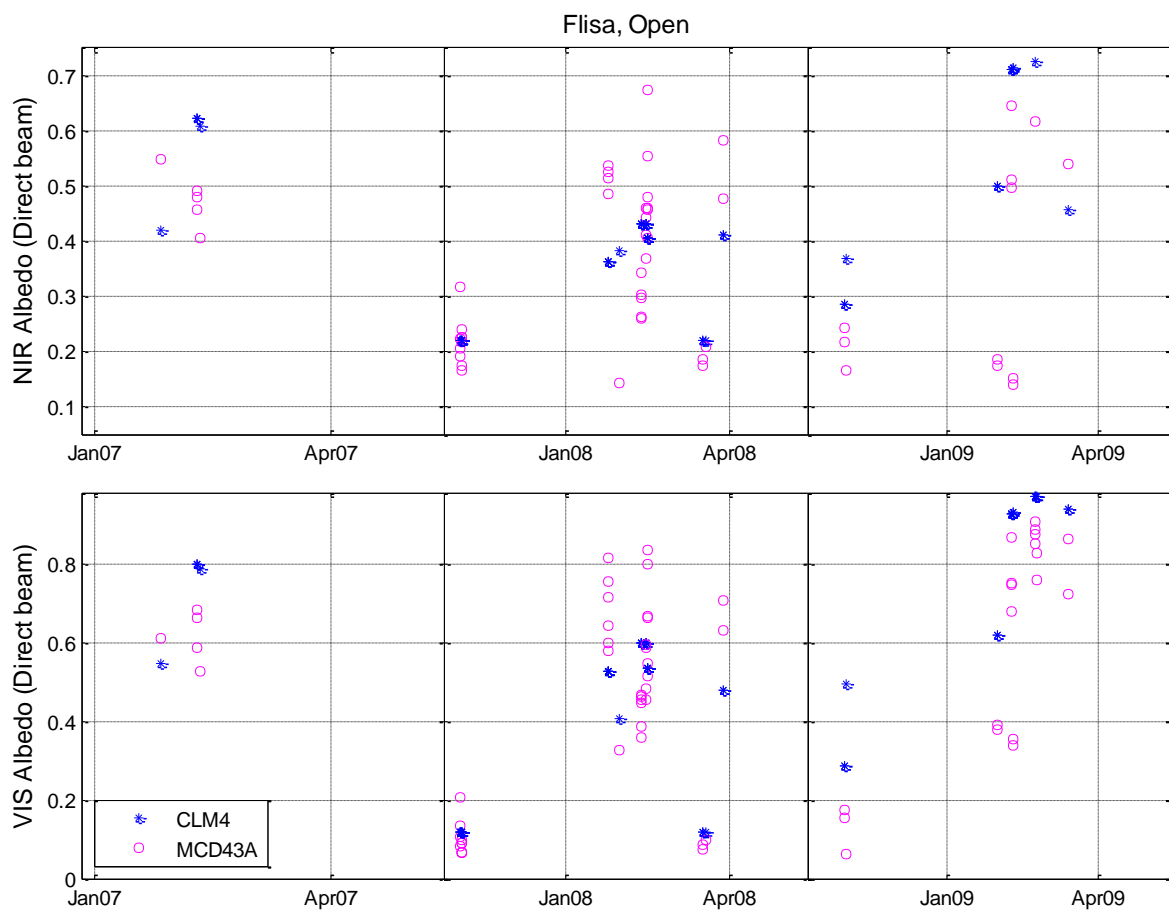


Figure S17. Predicted and observed daily black-sky albedo at the open area sites (cropland) in Flisa.

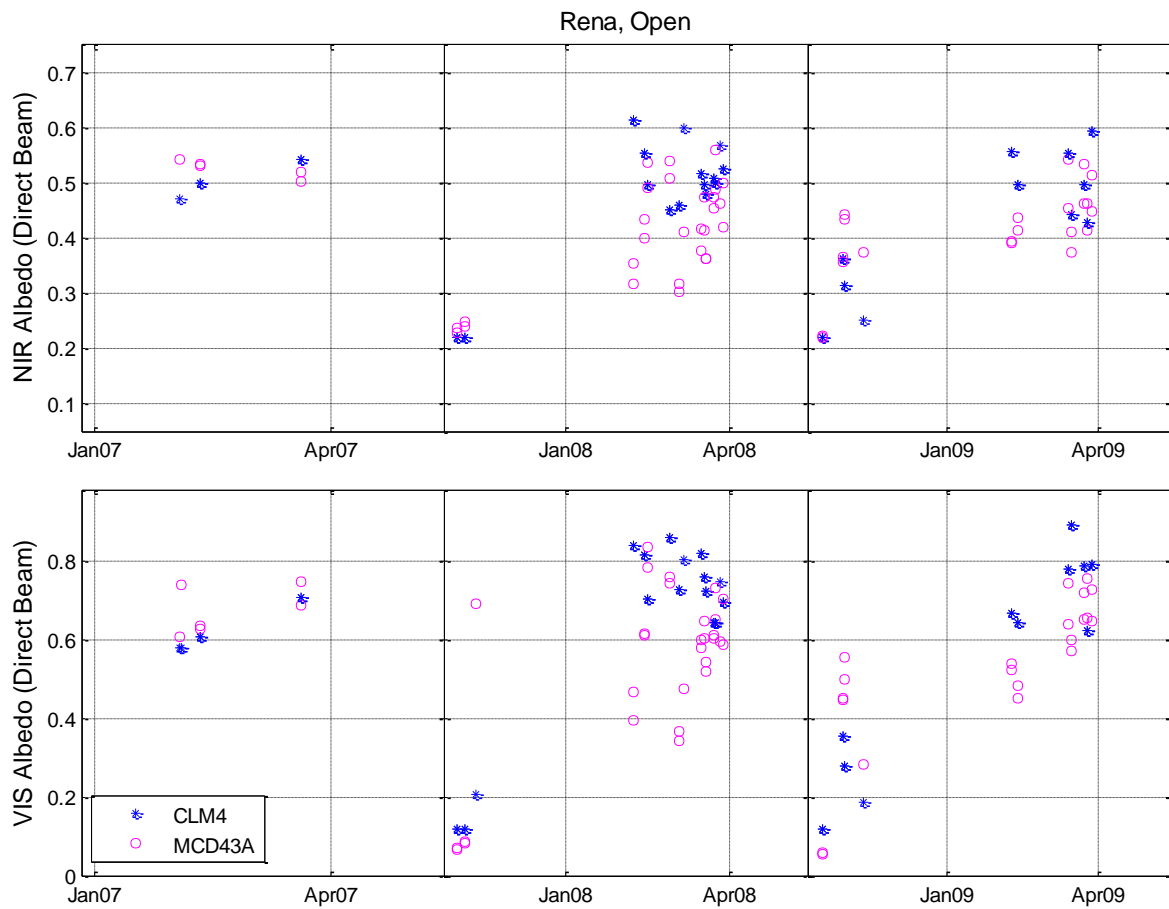


Figure S18. Predicted and observed daily black-sky albedo at the open area sites (cropland) in Rena.

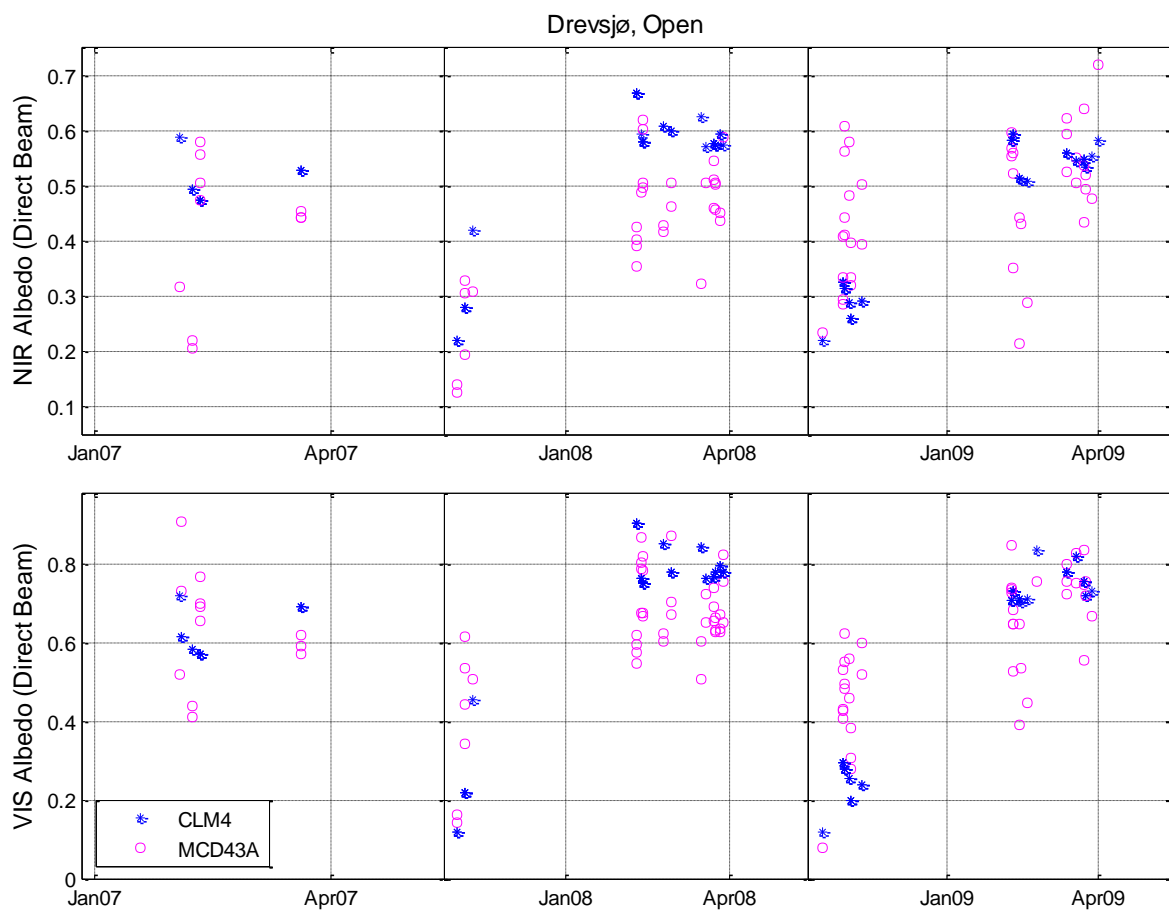


Figure S19. Predicted and observed daily black-sky albedo at the open area sites (wetland/peatland) in Drevsjø.

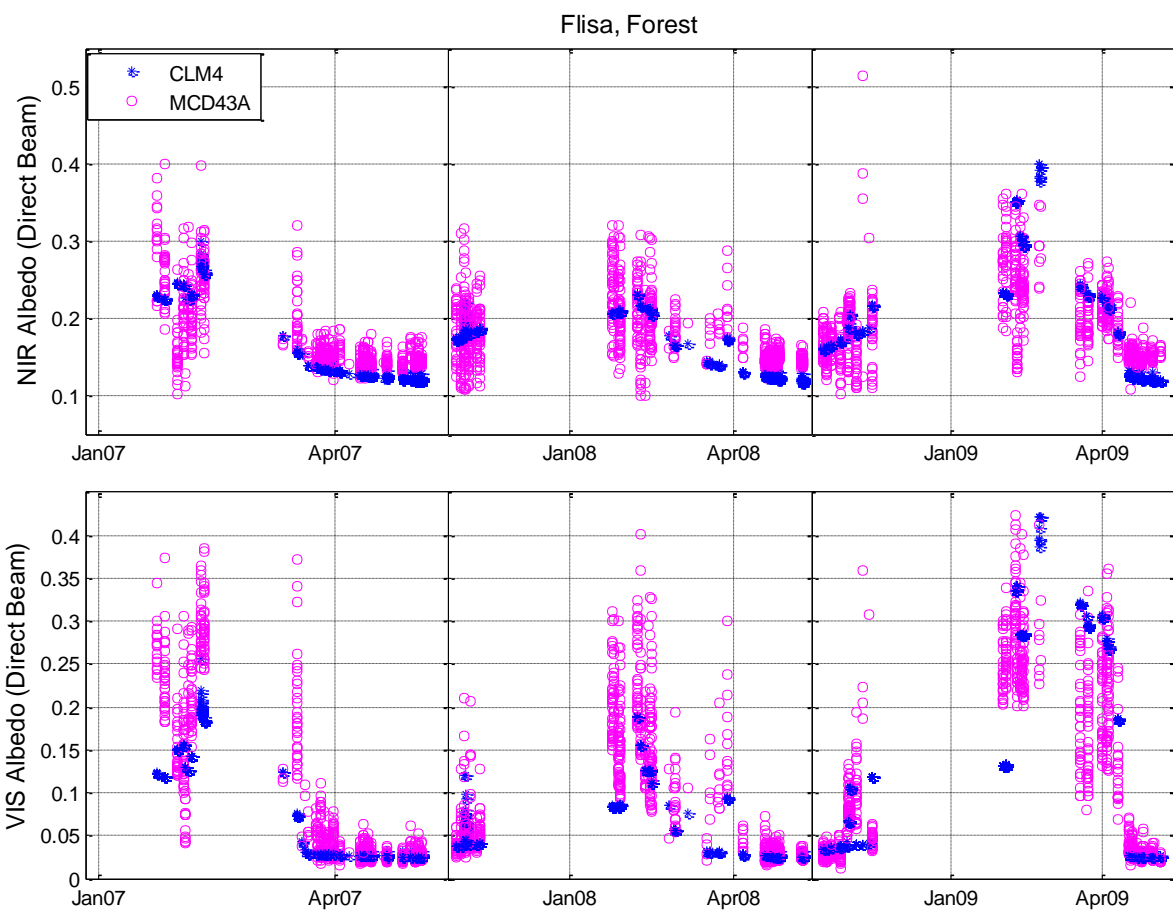


Figure S20. Predicted and observed daily black-sky albedo at the forested sites (evergreen needleleaf) in Flisa.

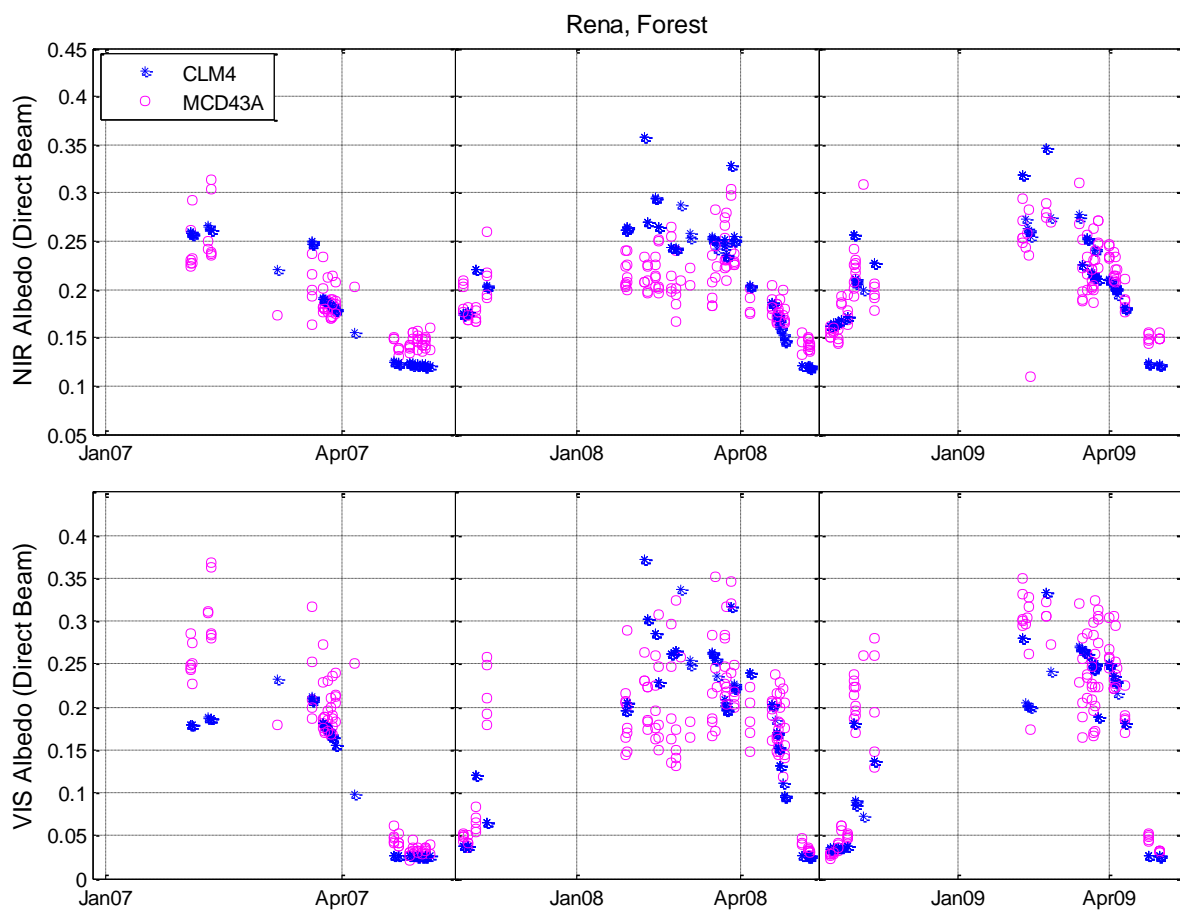


Figure S21. Predicted and observed daily black-sky albedo at the forested sites (evergreen needleleaf) in Rena.

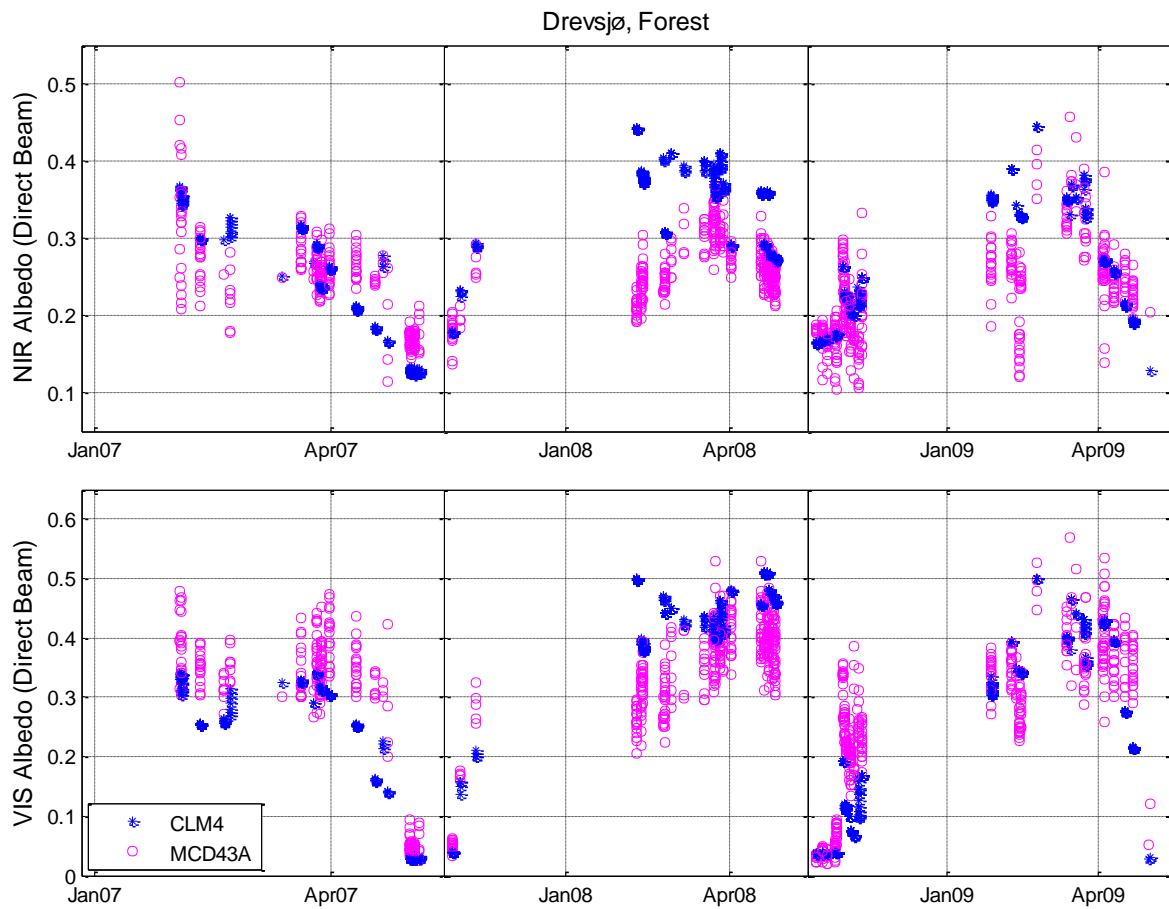


Figure S22. Predicted and observed daily black-sky albedo at the forested sites (evergreen needleleaf) in Drevsjø.

S.5.4. JSBACH

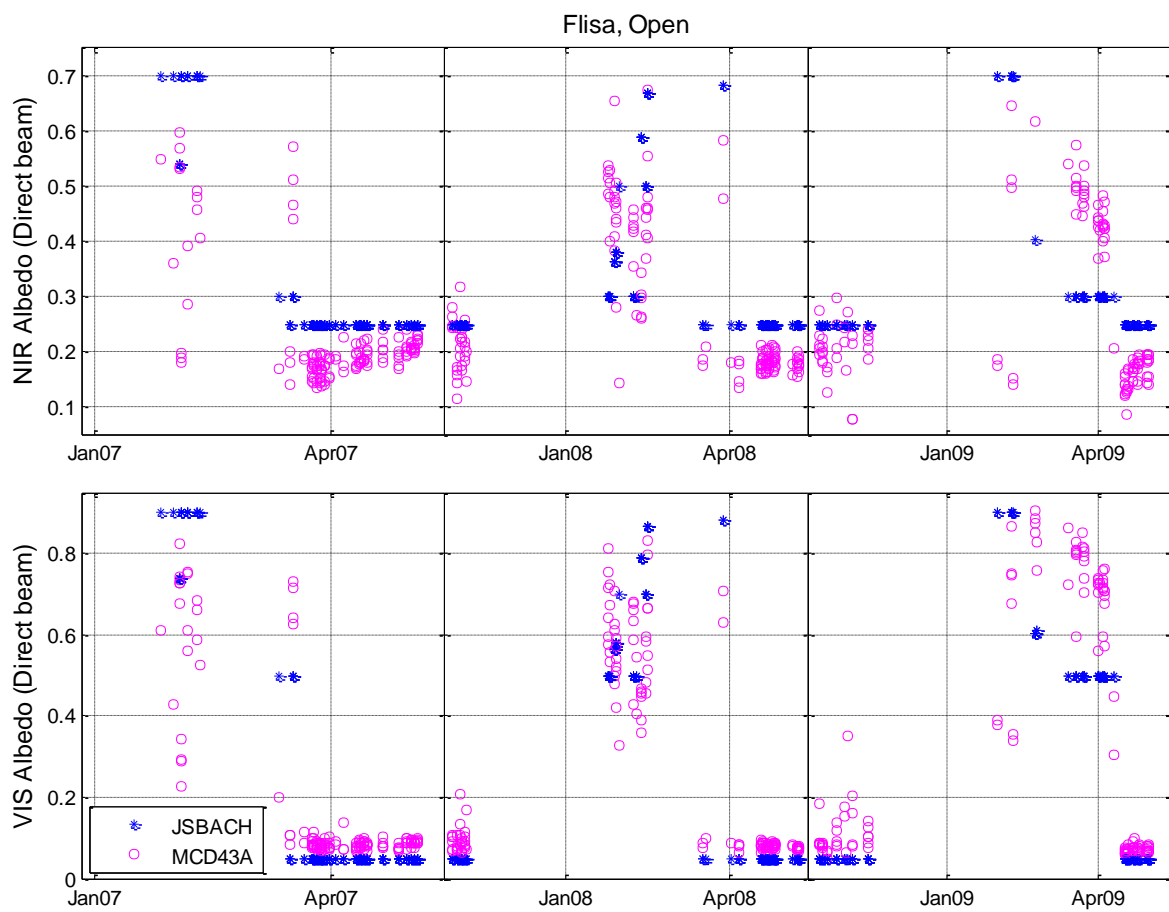


Figure S23. Predicted and observed daily black-sky albedo at the open area sites (cropland) in Flisa.

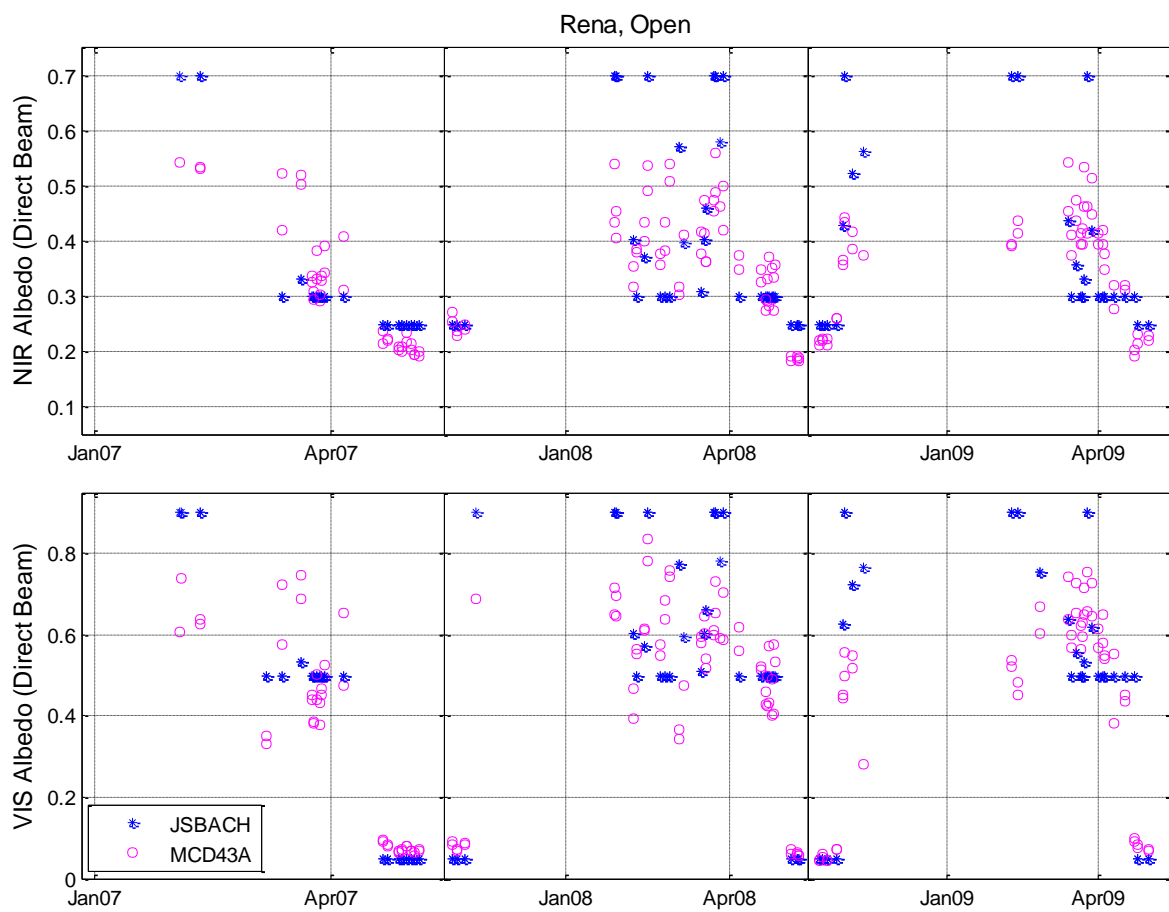


Figure S24. Predicted and observed daily black-sky albedo at the open area sites (cropland) in Rena.

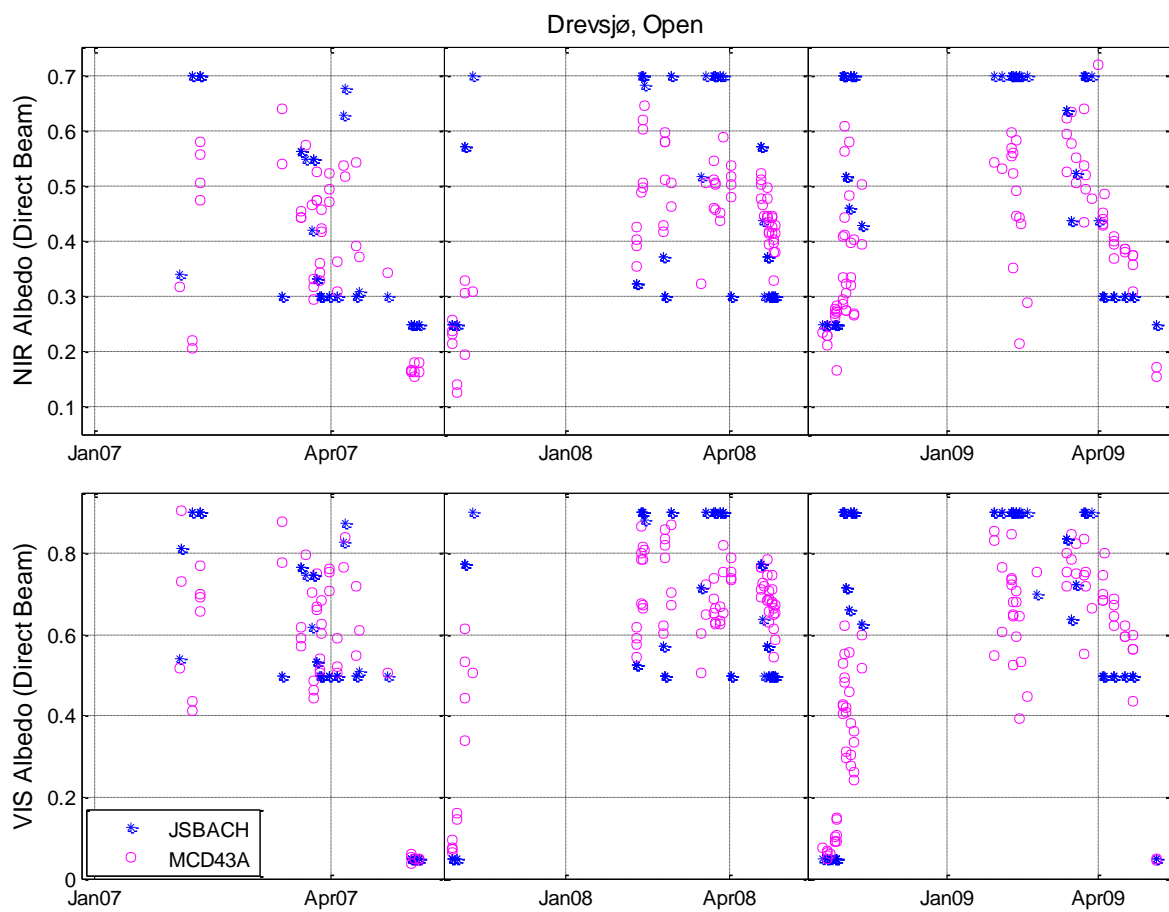


Figure S25. Predicted and observed daily black-sky albedo at the open area sites (wetland/peatland) in Drevsjø.

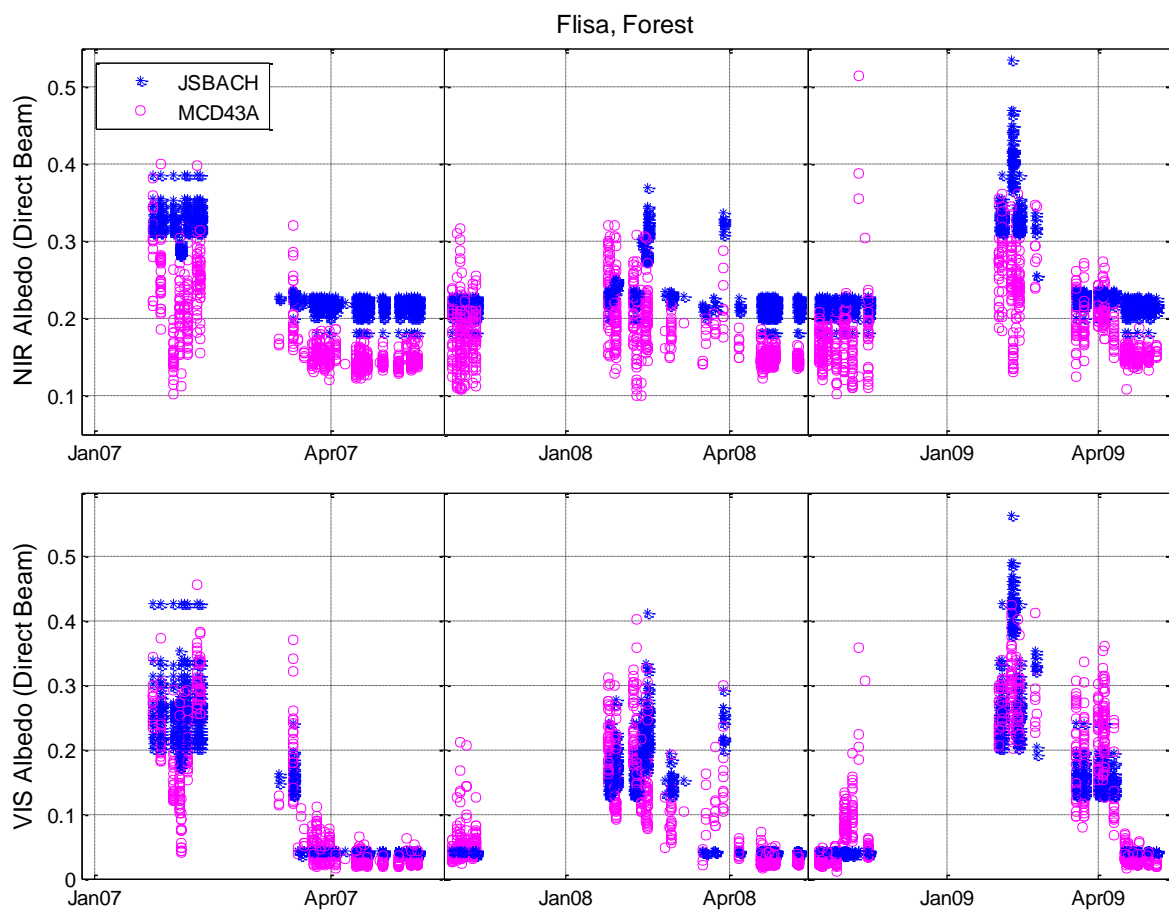


Figure S26. Predicted and observed daily black-sky albedo at the forested sites (evergreen needleleaf) in Flisa.

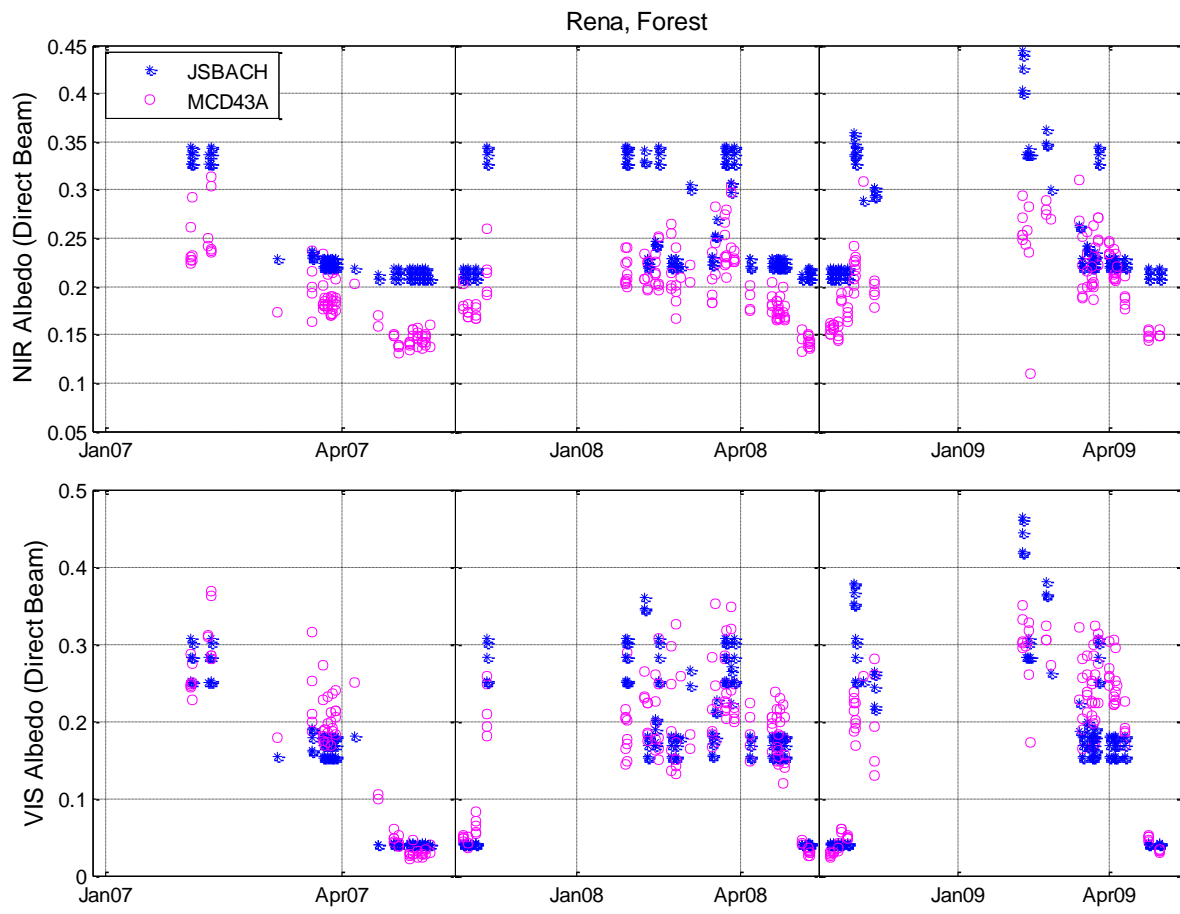


Figure S27. Predicted and observed daily black-sky albedo at the forested sites (evergreen needleleaf) in Rena.

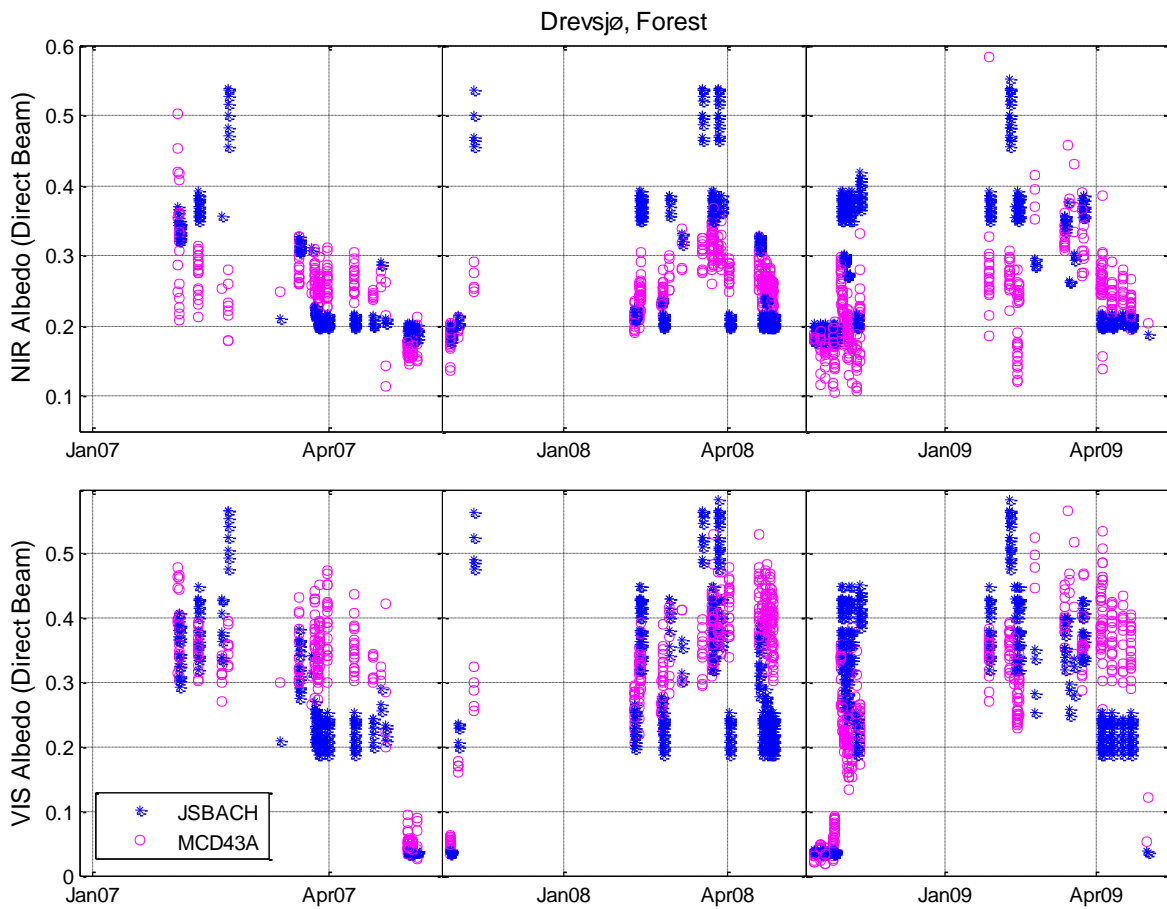


Figure S28. Predicted and observed daily black-sky albedo at the forested sites (evergreen needleleaf) in Drevsjø.

S.5.5. CLASS

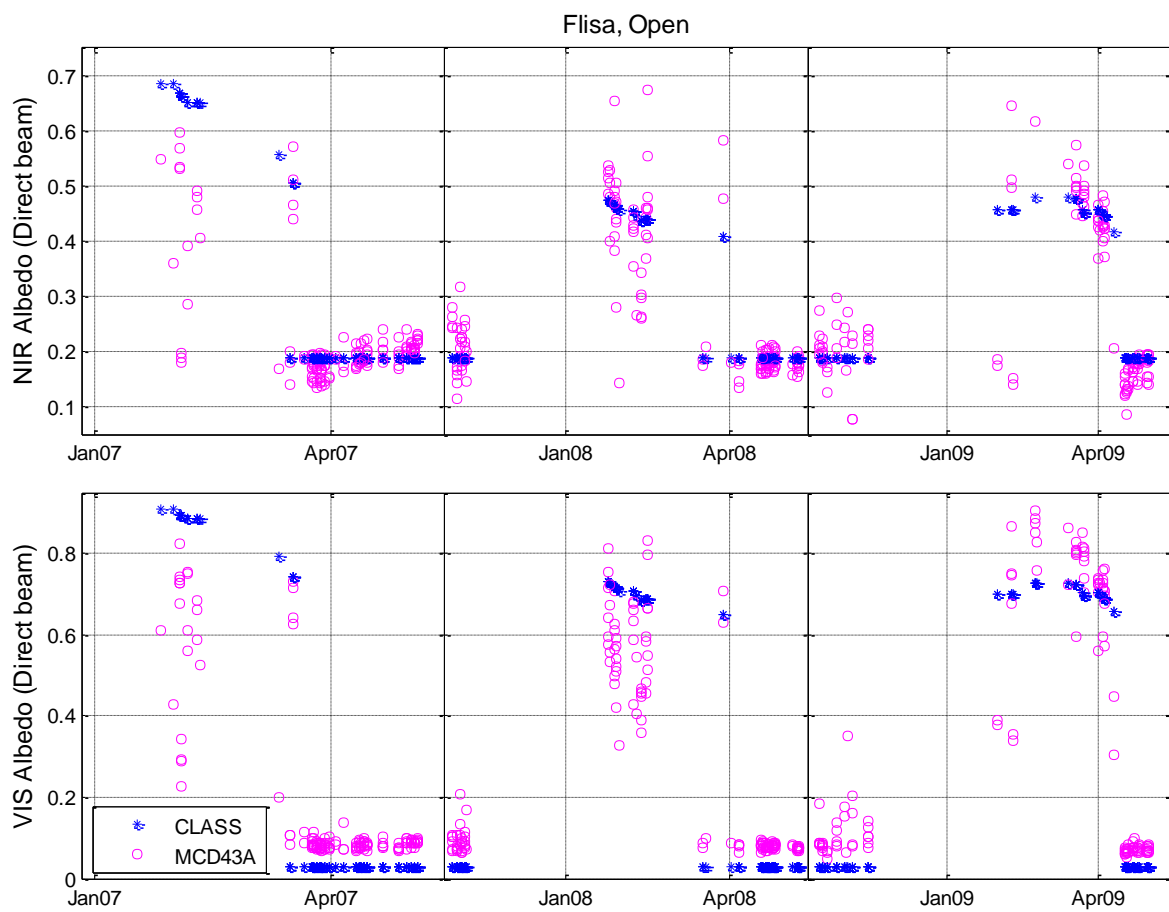


Figure S29. Predicted and observed daily black-sky albedo at the open area sites (cropland) in Flisa.

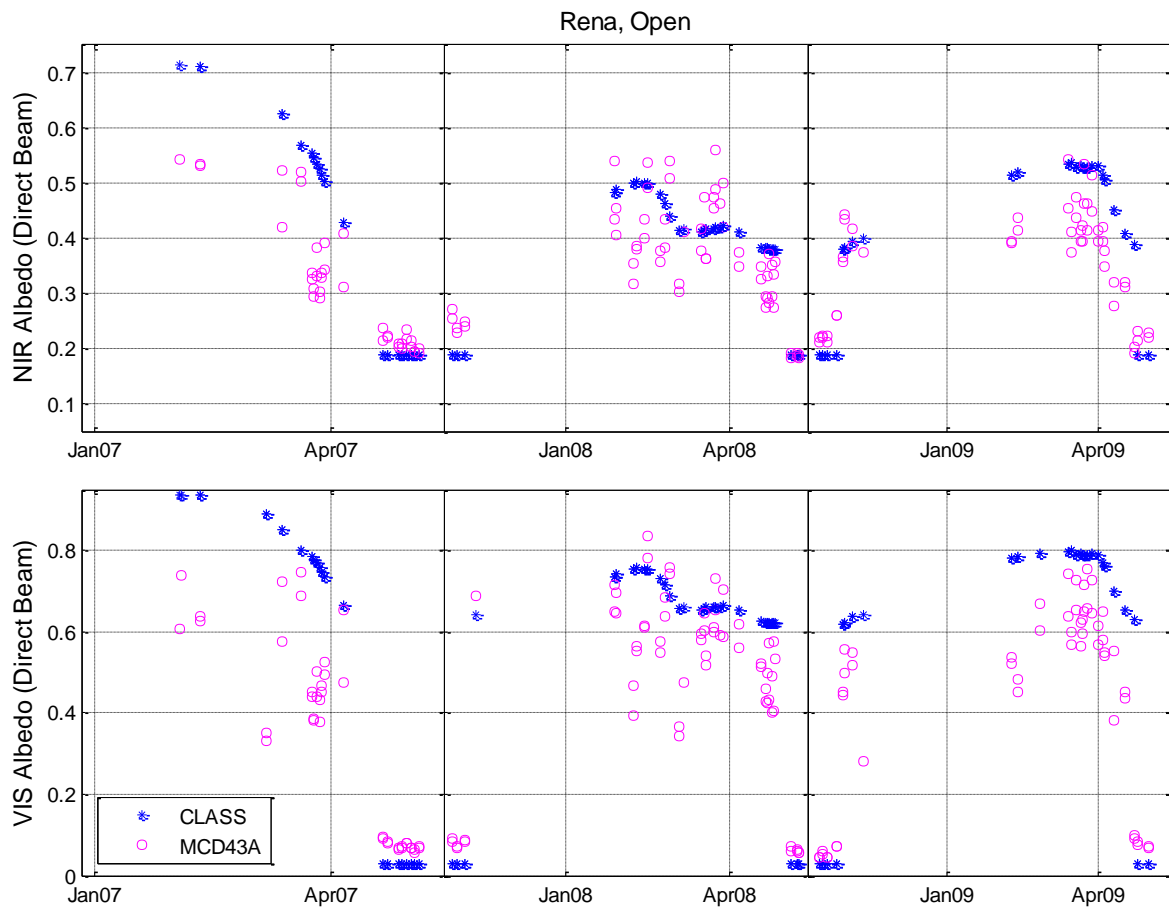


Figure S30. Predicted and observed daily black-sky albedo at the open area sites (cropland) in Rena.

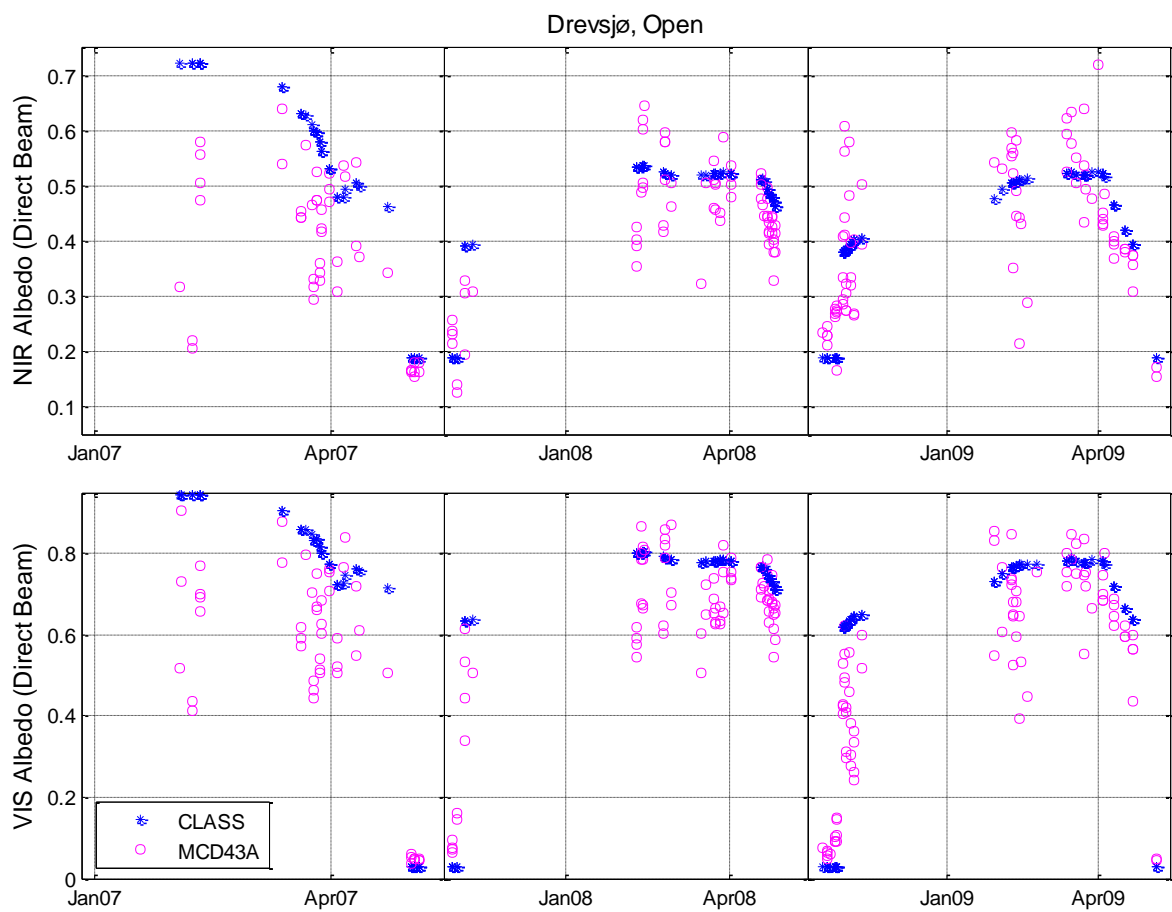


Figure S31. Predicted and observed daily black-sky albedo at the open area sites (wetland/peatland) in Drevsjø.

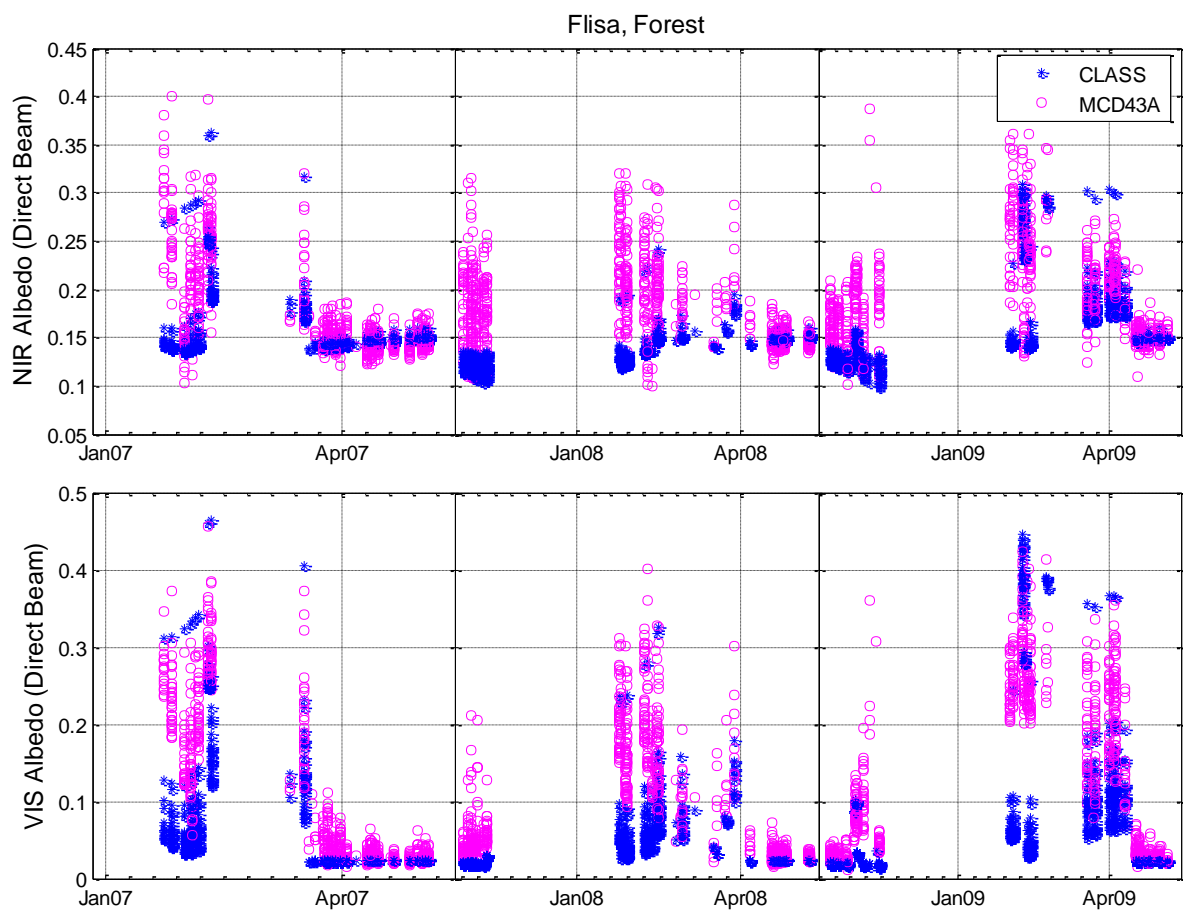


Figure S32. Predicted and observed daily black-sky albedo at the forested sites (evergreen needleleaf) in Flisa.

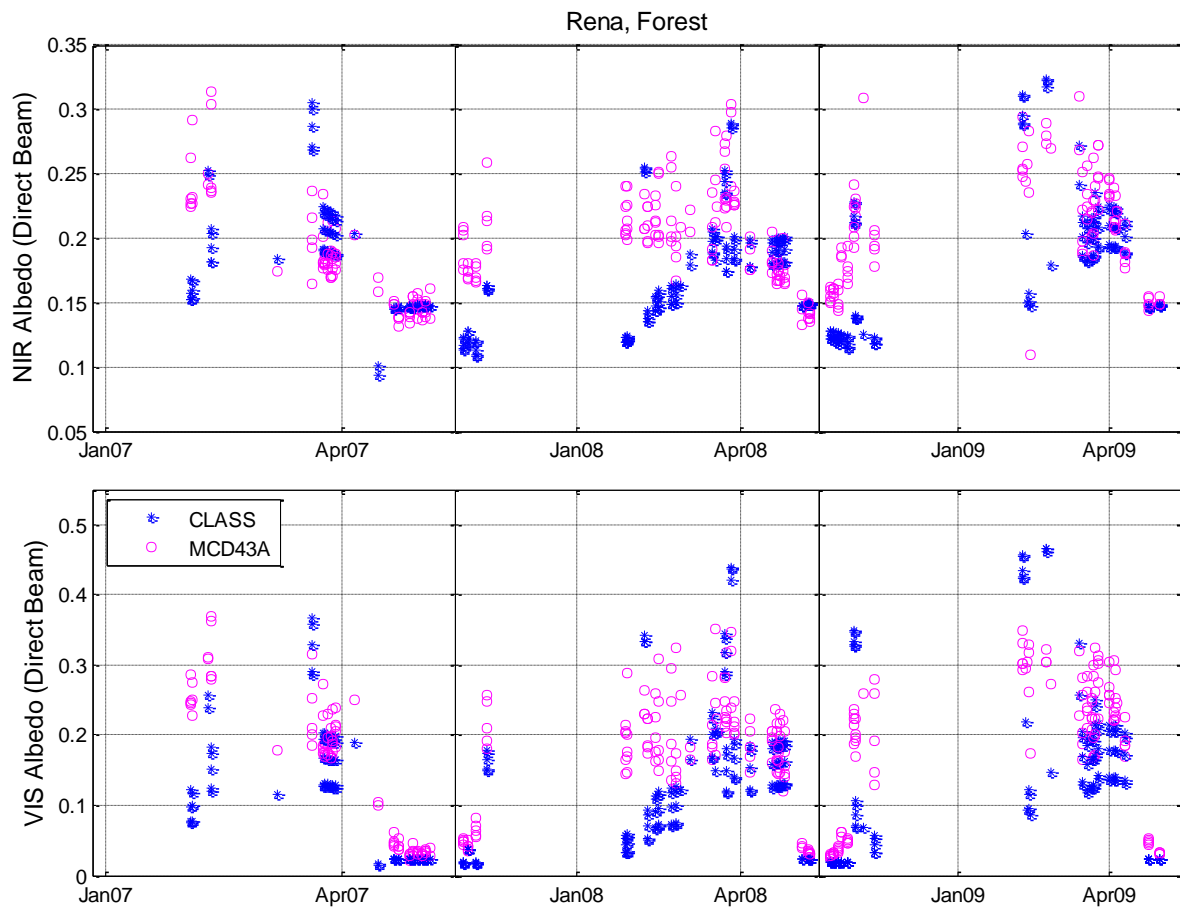


Figure S33. Predicted and observed daily black-sky albedo at the forested sites (evergreen needleleaf) in Rena.

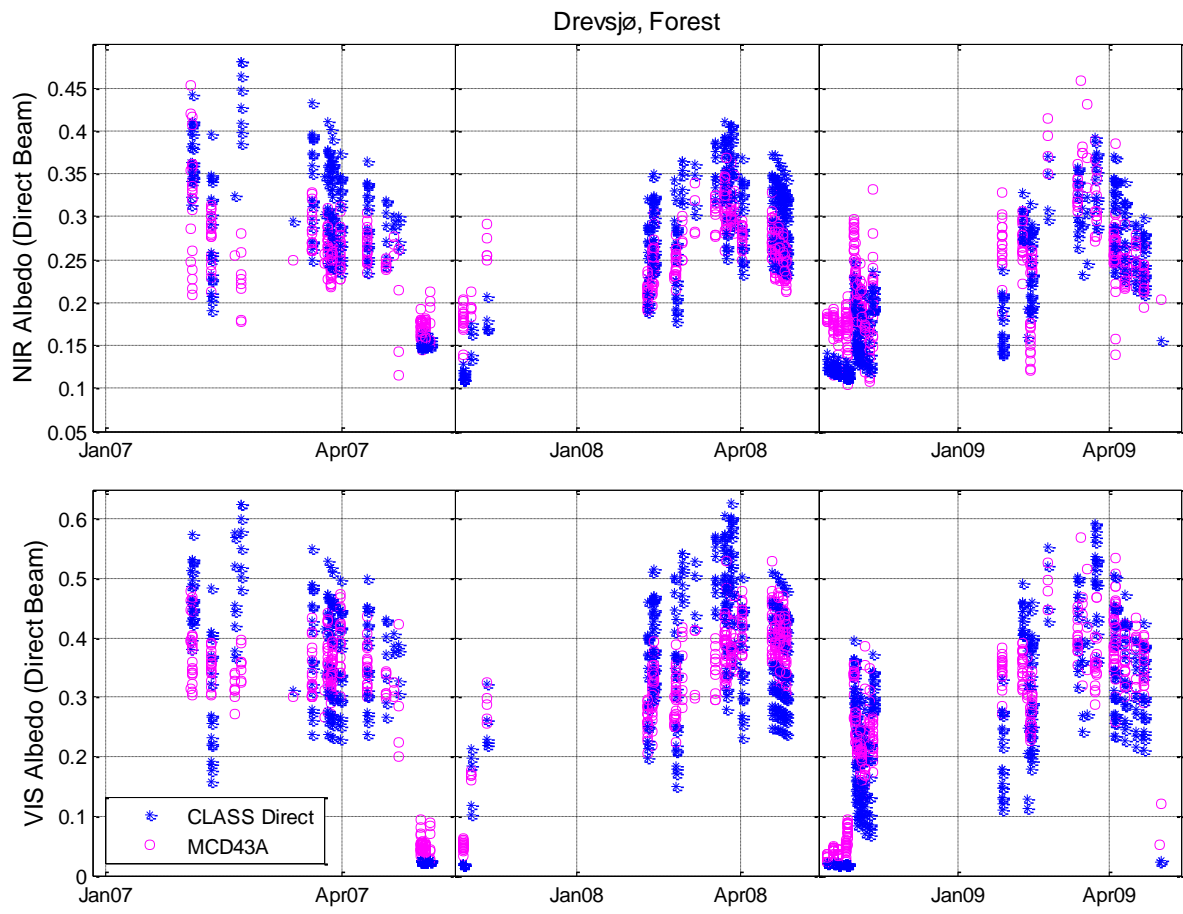


Figure S34. Predicted and observed daily black-sky albedo at the forested sites (evergreen needleleaf) in Drevsjø.

S.5.6. GISS II

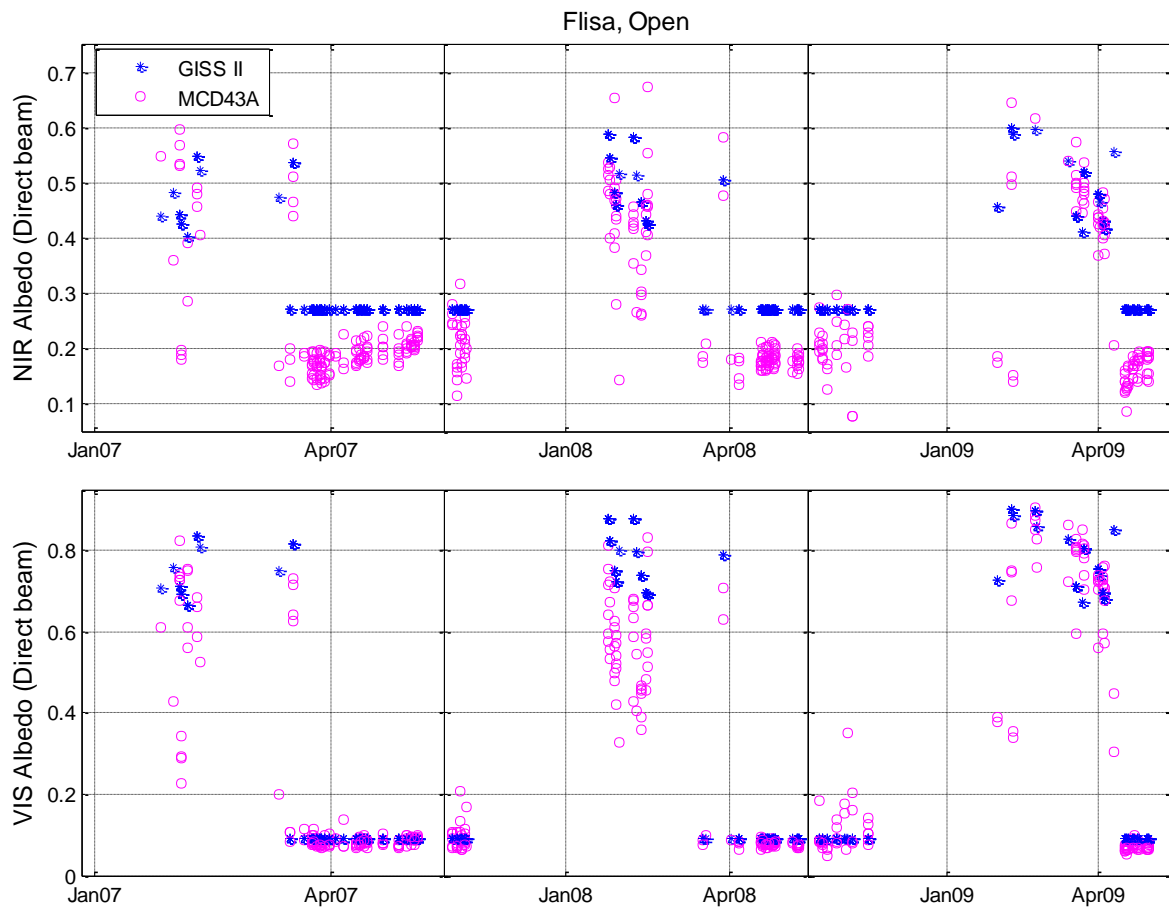


Figure S35. Predicted and observed daily black-sky albedo at the open area sites (cropland) in Flisa.

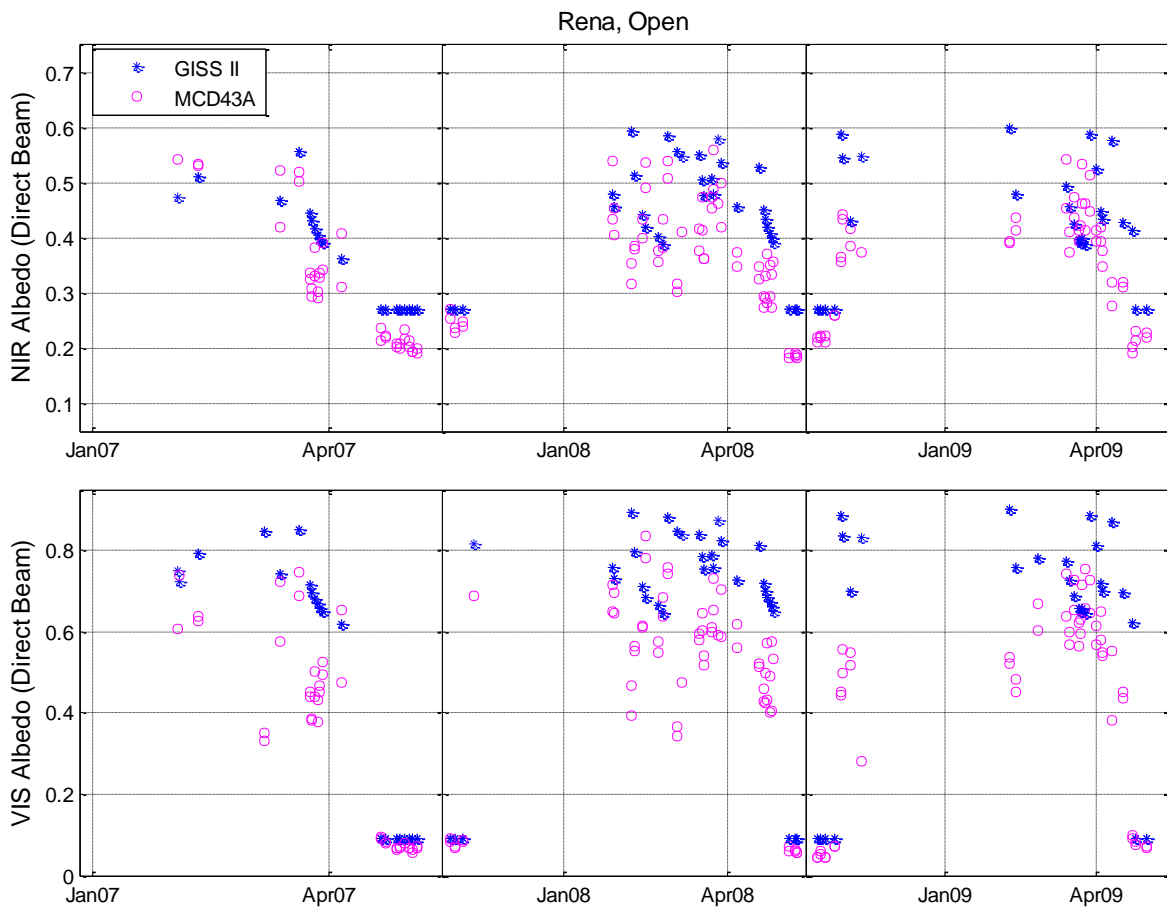


Figure S36. Predicted and observed daily black-sky albedo at the open area sites (cropland) in Rena.

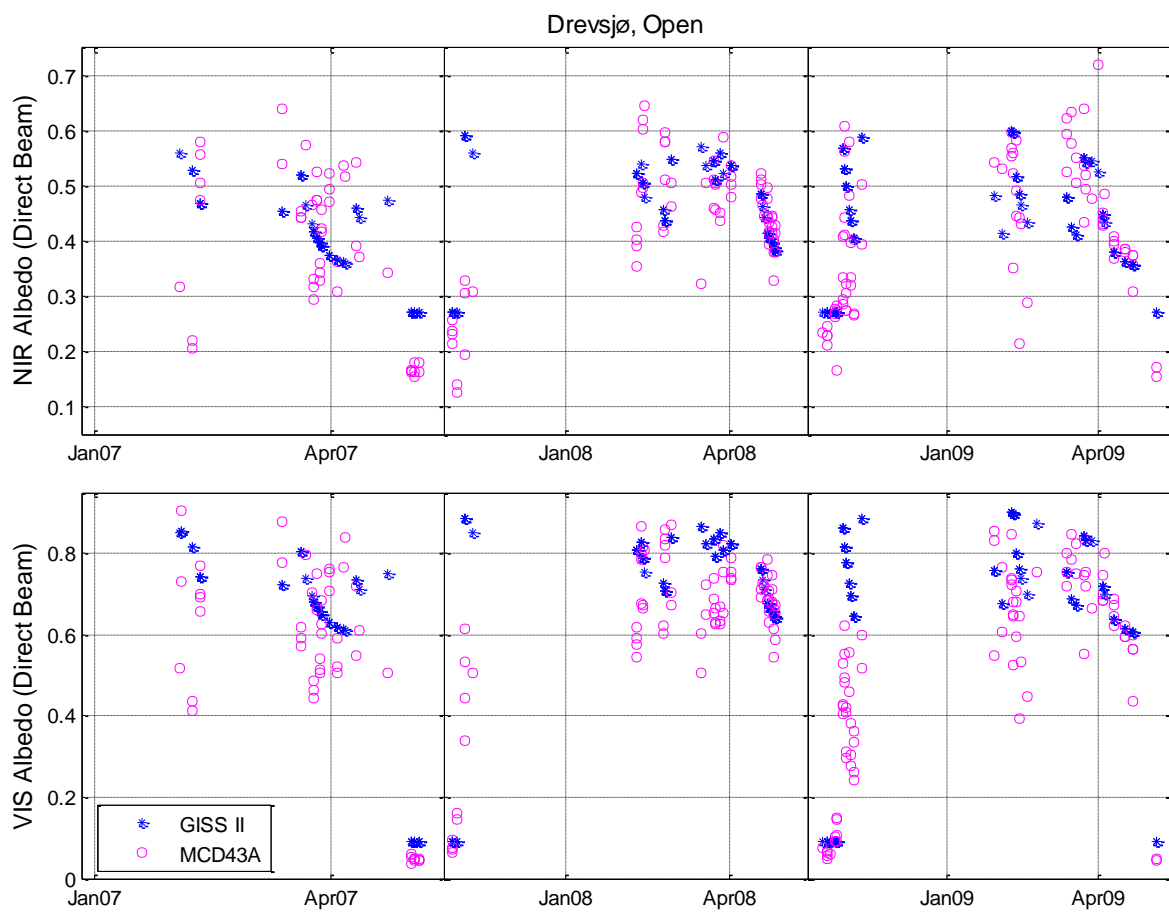


Figure S37. Predicted and observed daily black-sky albedo at the open area sites (wetland/peatland) in Flisa.

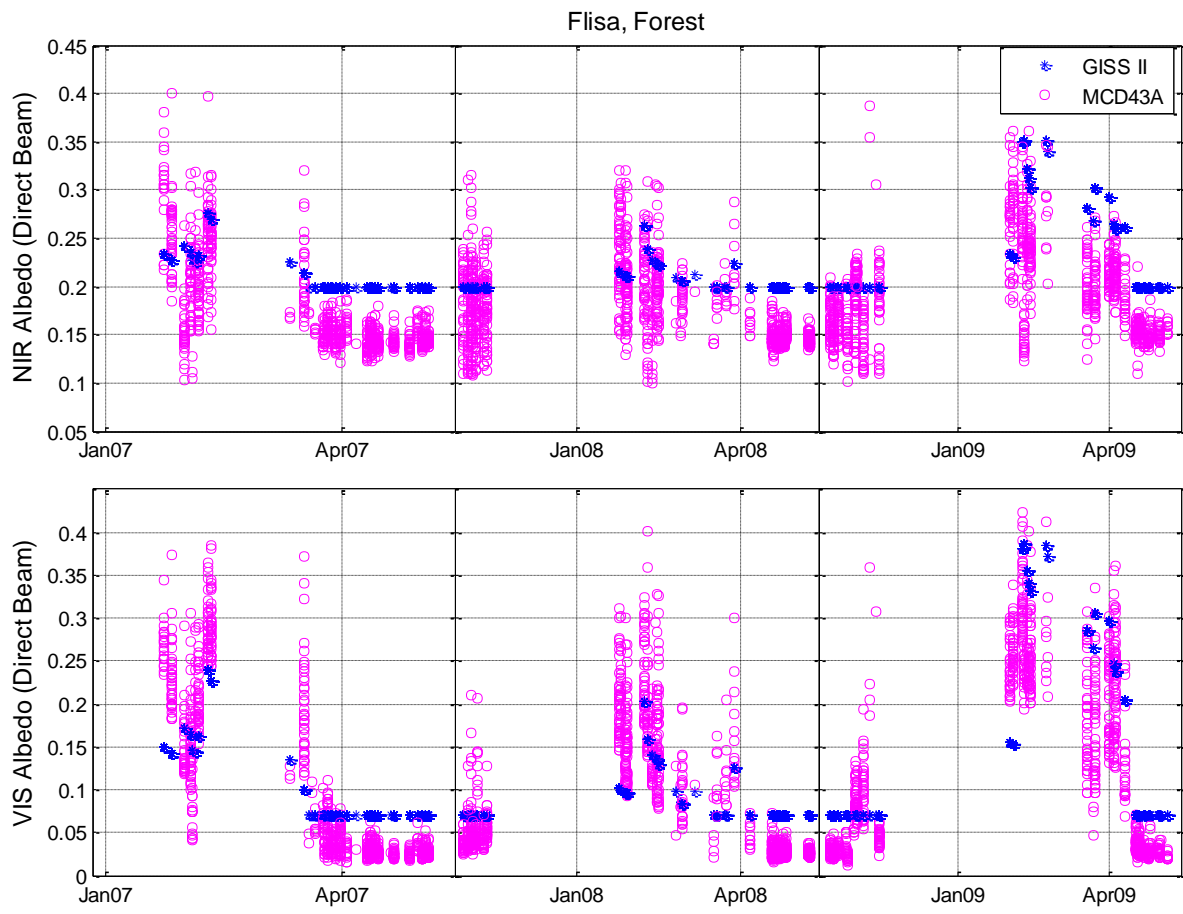


Figure S38. Predicted and observed daily black-sky albedo at the forested sites (evergreen needleleaf) in Flisa.

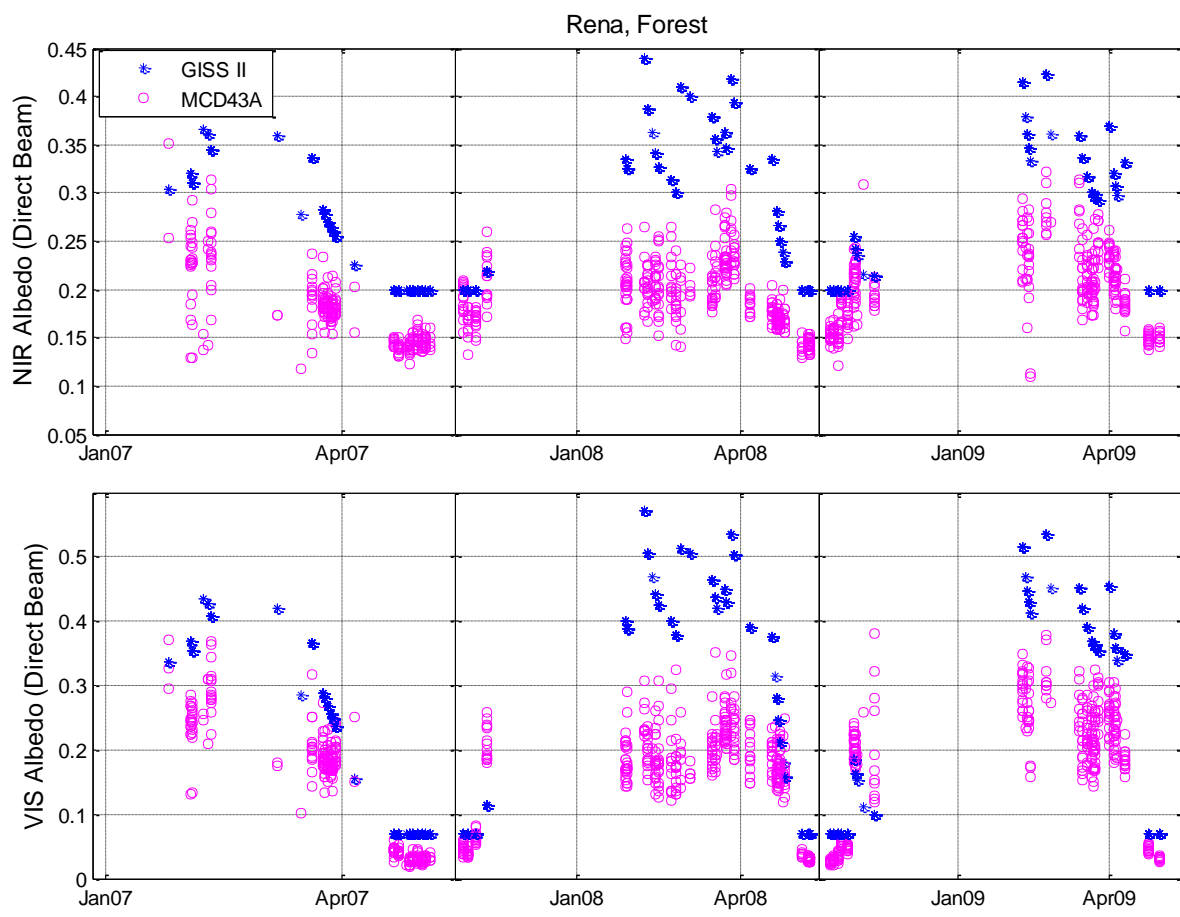


Figure S39. Predicted and observed daily black-sky albedo at the forested sites (evergreen needleleaf) in Rena.

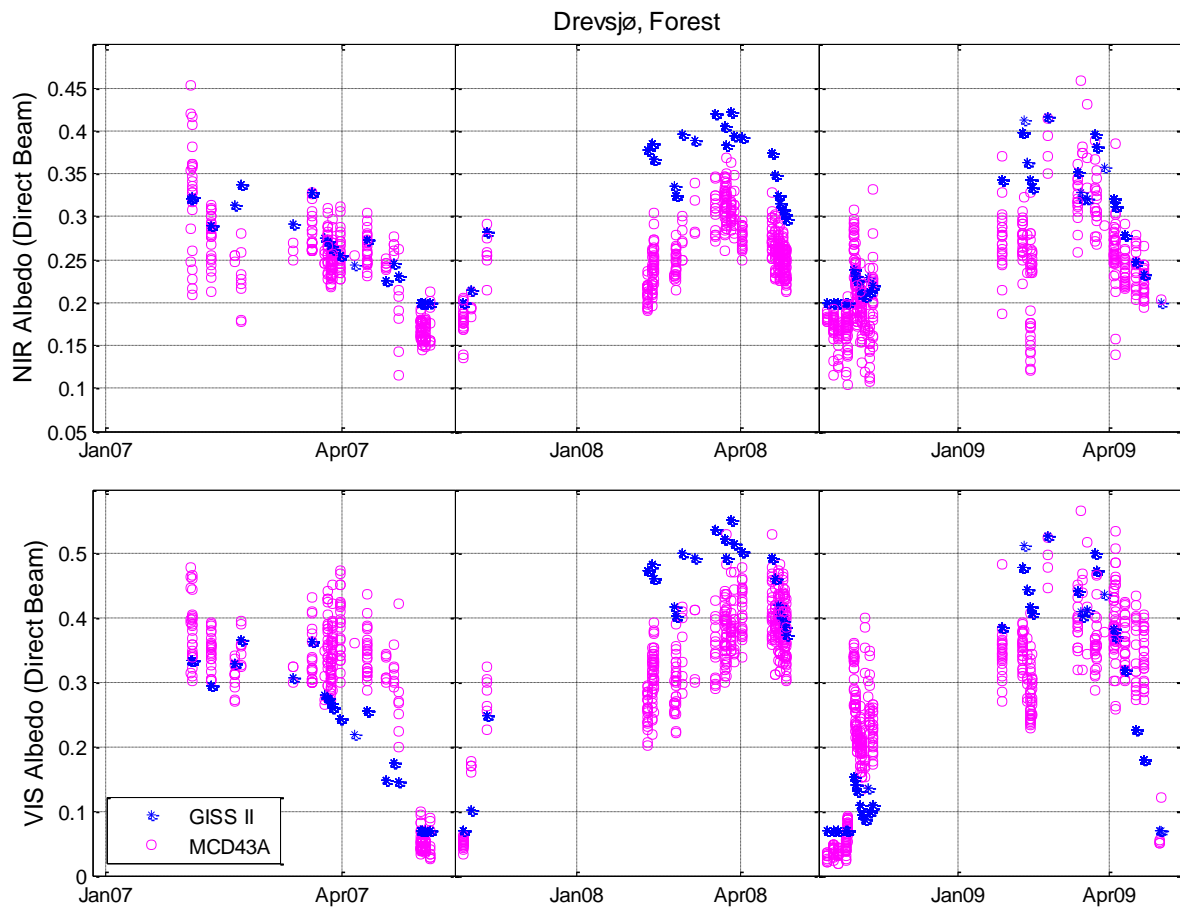


Figure S40. Predicted and observed daily black-sky albedo at the forested sites (evergreen needleleaf) in Drevsjø.

S.5.7. Regression model

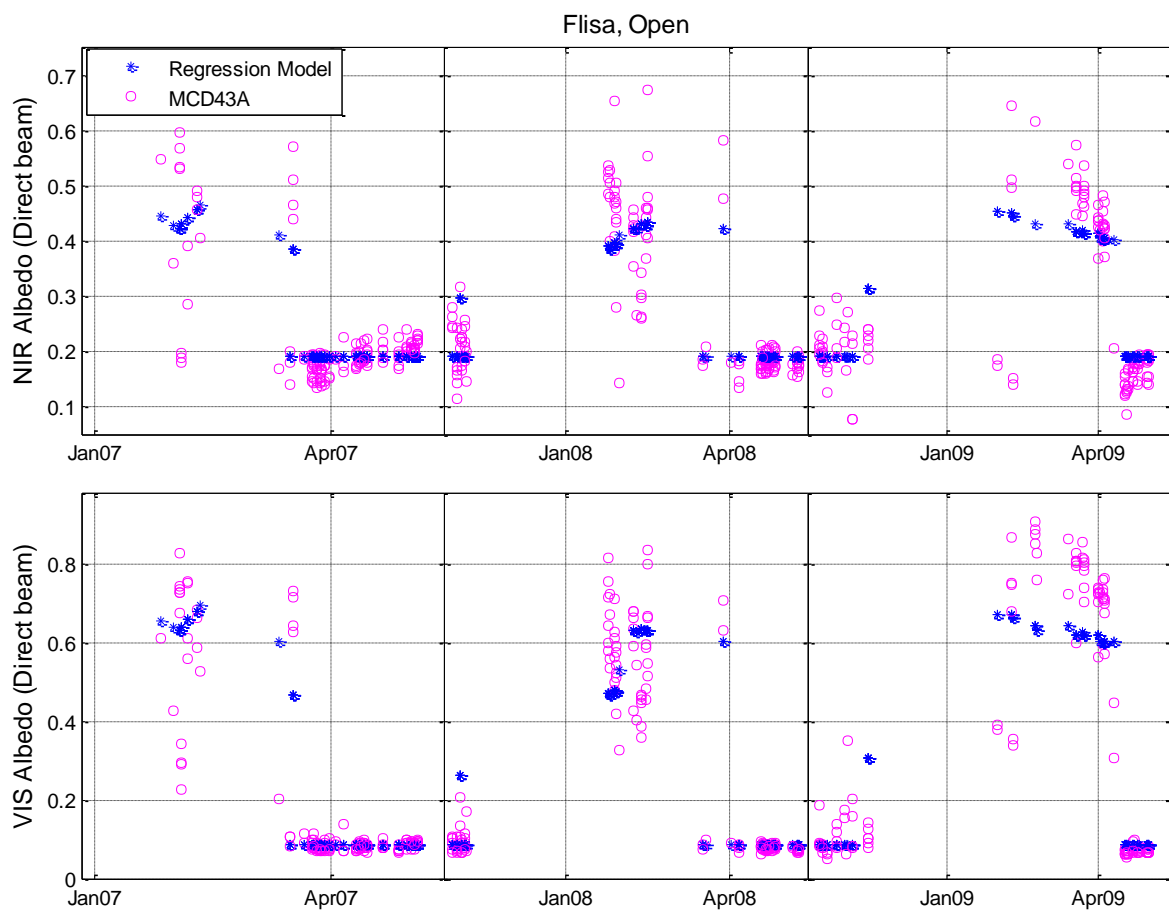


Figure S41. Predicted and observed daily black-sky albedo at the open area sites (cropland) in Flisa.

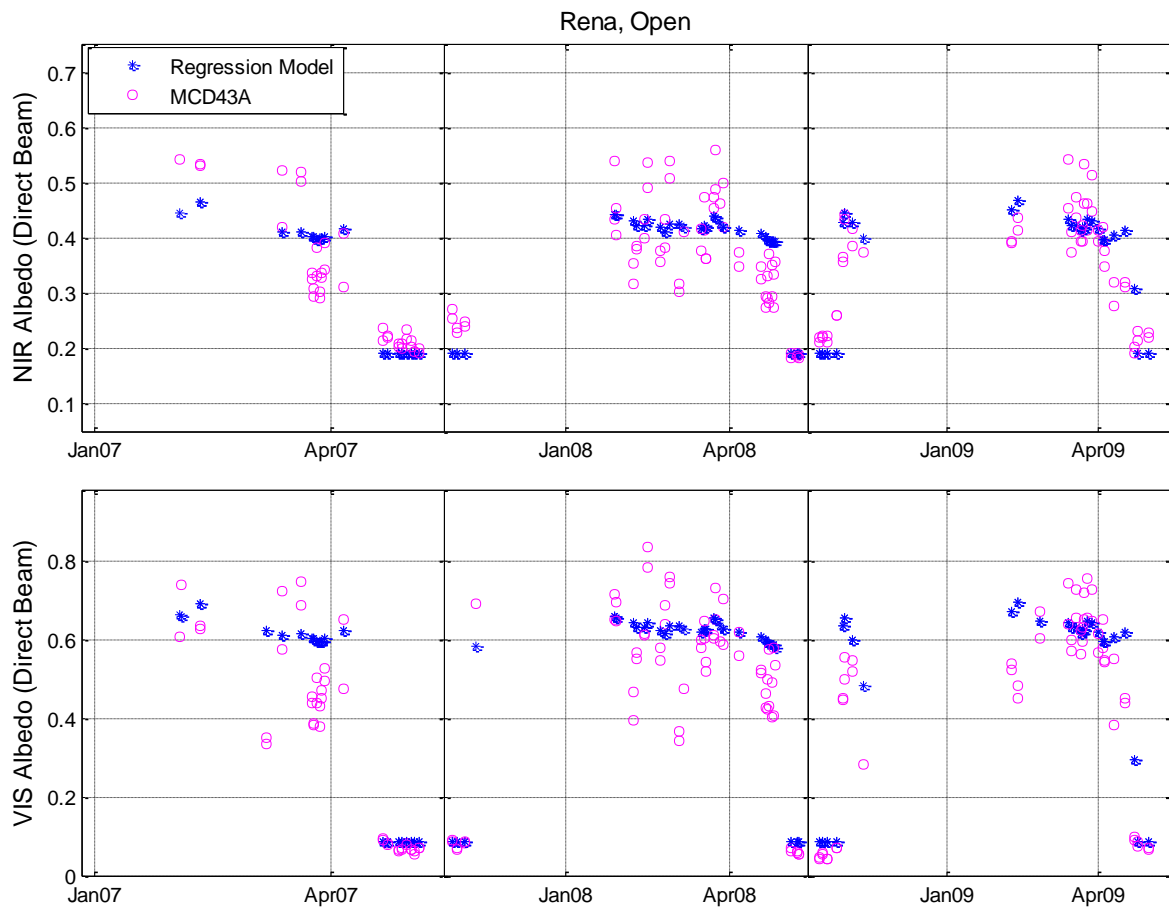


Figure S42. Predicted and observed daily black-sky albedo at the open area sites (cropland) in Rena.

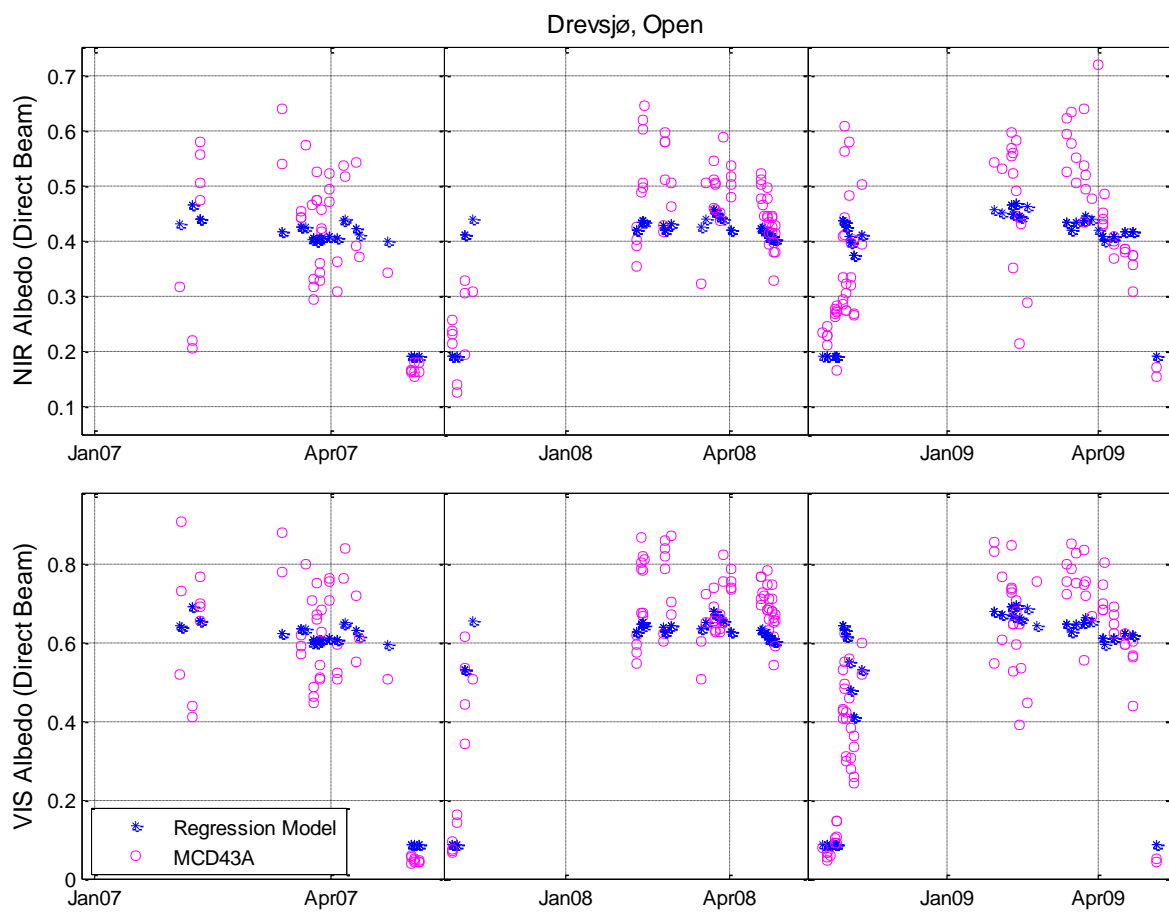


Figure S43. Predicted and observed daily black-sky albedo at the open area sites (wetland/peatland) in Drevsjø.

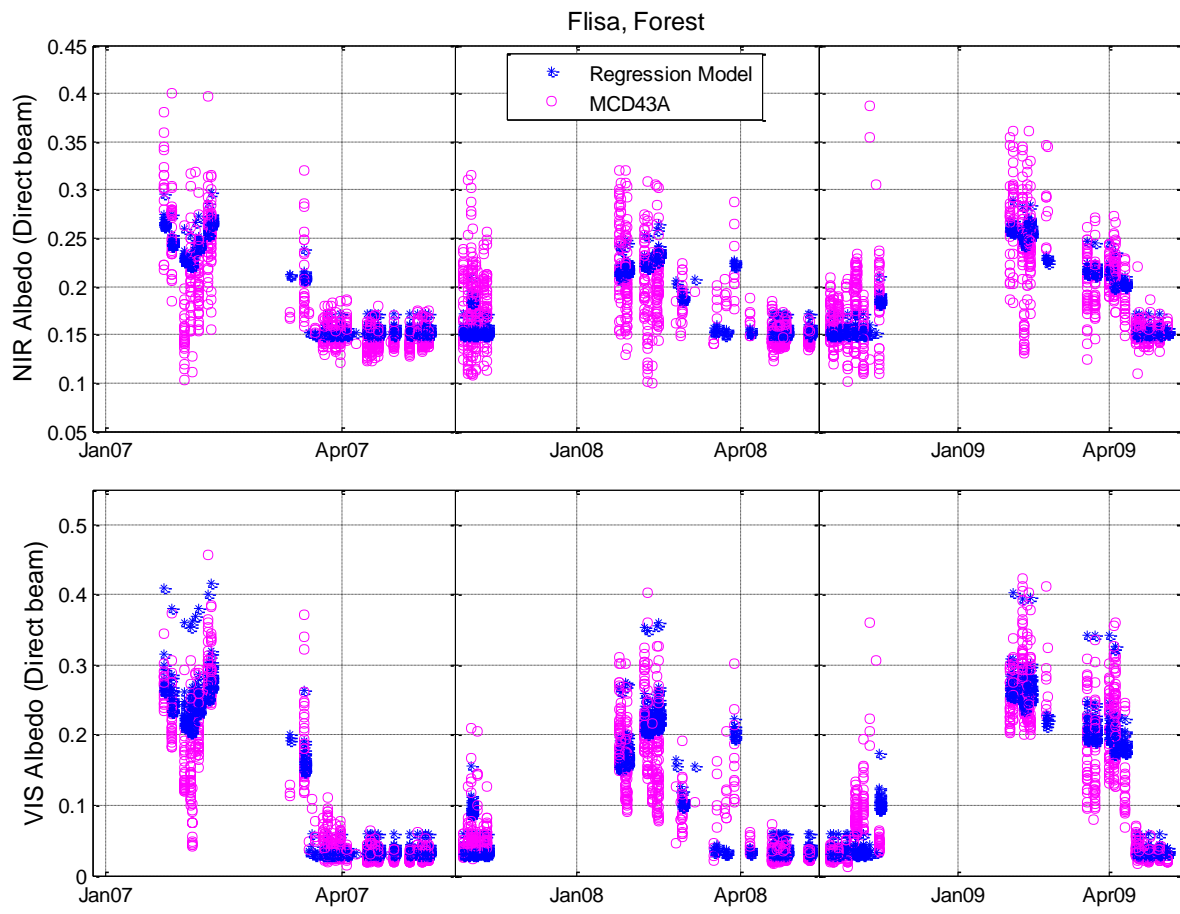


Figure S44. Predicted and observed daily black-sky albedo at the forested sites (evergreen needleleaf) in Flisa.

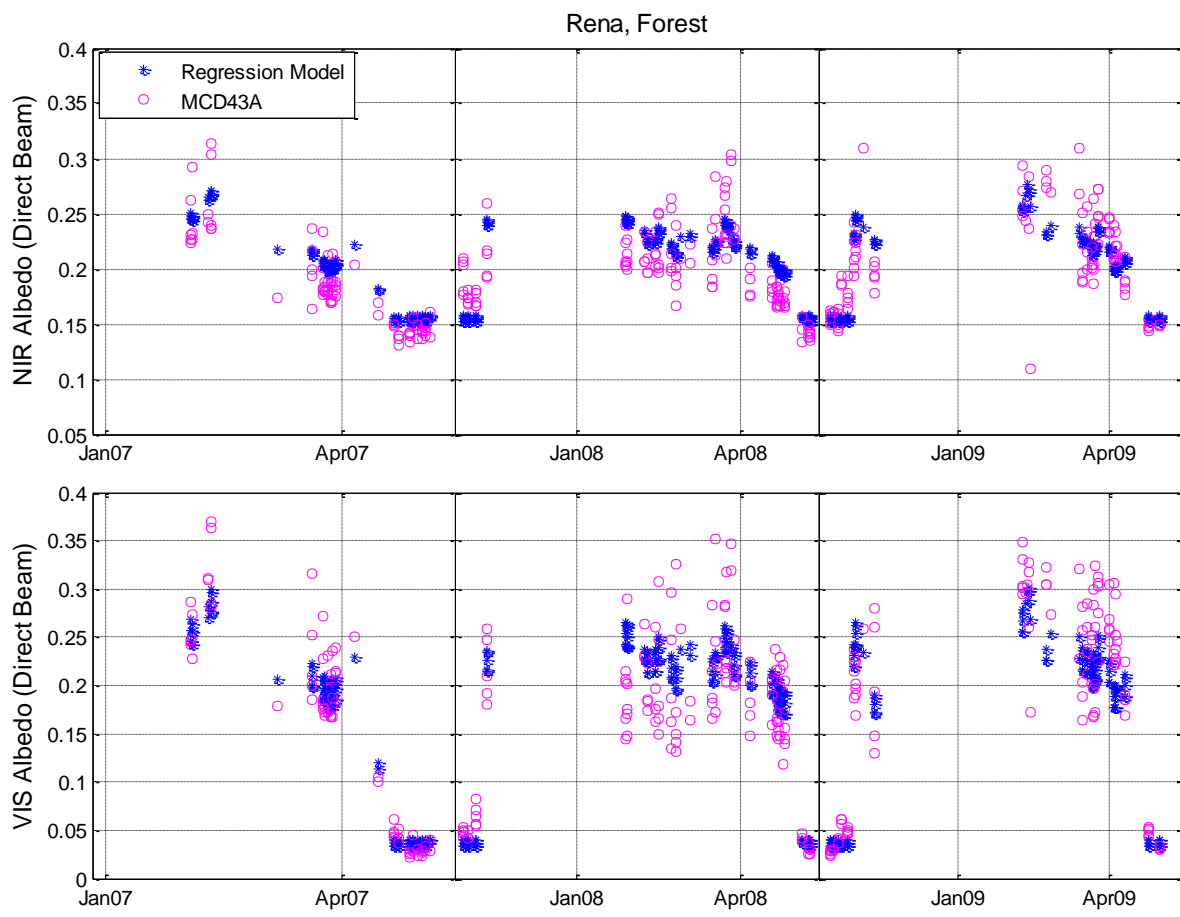


Figure S45. Predicted and observed daily black-sky albedo at the forested sites (evergreen needleleaf) in Rena.

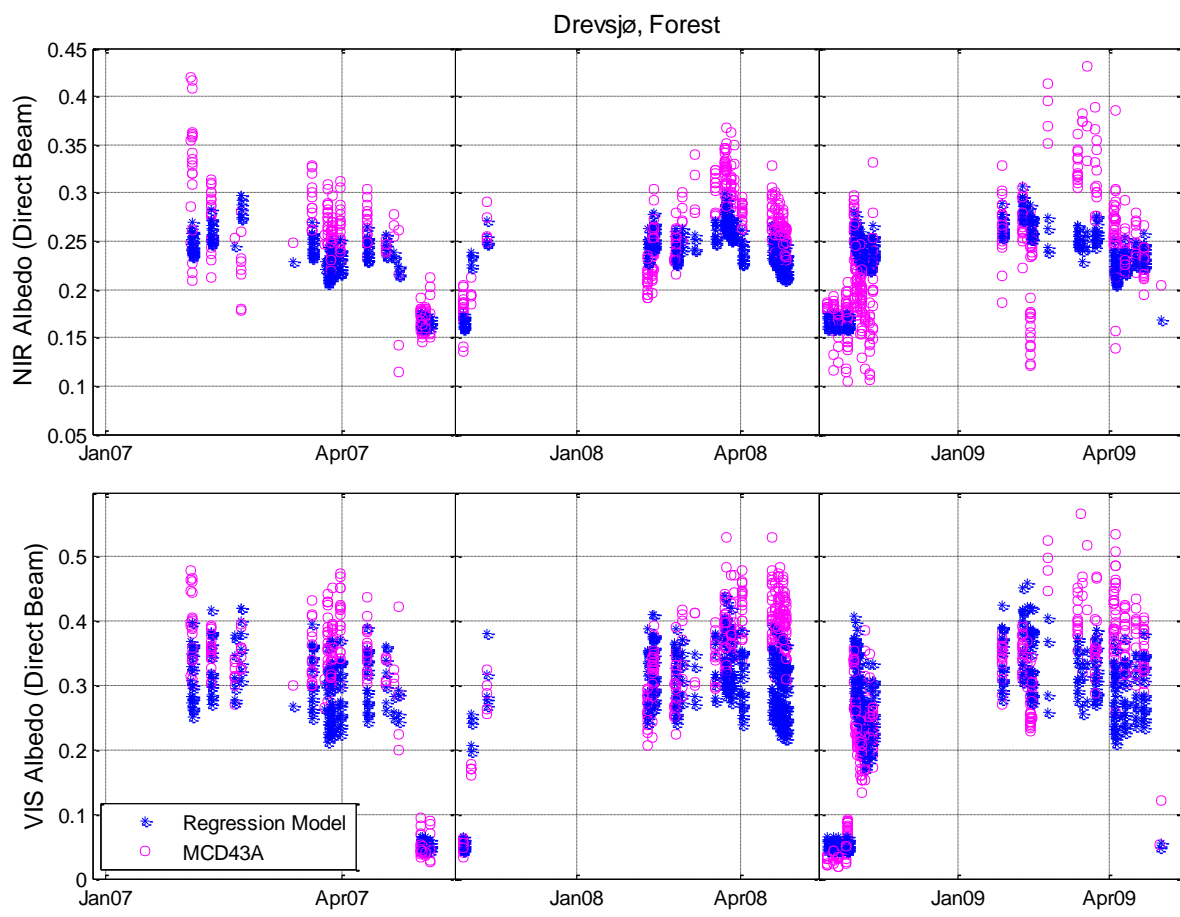


Figure S46. Predicted and observed daily black-sky albedo at the forested sites (evergreen needleleaf) in Drevsjø.

Table S6. Mean bias^a, 2007-2009 Nov.-May mean and solar insolation-weighted mean $\Delta\alpha$ (Open – Forest). High solar zenith angles inhibit the number of sufficient MODIS observations in December, thus December is excluded from the calculations.

Model	NIR		VIS	
	Mean (Nov.- May)	Insolation- weighted Mean (Nov.-May)	Mean (Nov.- May)	Insolation- weighted Mean (Nov.-May)
	$\Delta\alpha$, Flisa (60.6° N, 12.0° W)			
Regression	0.01	0.00	0.00	0.00
JULES 2-stream	0.01	-0.01	0.07	0.04
CLM4	0.03	0.01	0.05	0.01
JSBACH	0.01	0.00	0.01	-0.03
CLASS	0.08	0.04	0.10	0.02
JULES All-band	-0.02	-0.02	-0.02	-0.01
GISS II	0.05	0.04	0.08	0.01
$\Delta\alpha$, Rena (61.2° N, 11.4° W)				
Regression	-0.01	0.00	0.03	0.04
JULES 2-stream	-0.08	-0.06	0.01	0.03
CLM4	0.01	0.03	0.04	0.05
JSBACH	0.00	-0.02	0.07	0.03
CLASS	0.07	0.04	0.16	0.11
JULES All-band	0.03	0.00	0.05	0.04
GISS II	-0.02	-0.01	0.03	0.02
$\Delta\alpha$, Drevsjø (61.9° N, 12.1° W)				
Regression	-0.01	0.01	0.01	0.03
JULES 2-stream	-0.07	-0.05	0.05	0.06
CLM4	-0.01	-0.02	0.02	0.03
JSBACH	0.05	0.03	0.09	0.05
CLASS	0.05	0.04	0.10	0.08
JULES All-band	0.06	0.05	0.12	0.10
GISS II	-0.01	0.01	0.05	0.04
$\Delta\alpha$, Regional Mean (also shown in Figure 1 of main article)				
Regression	0.00	0.01	0.02	0.03
JULES 2-stream	-0.05	-0.04	0.05	0.04
CLM4	0.01	0.01	0.04	0.03
JSBACH	0.02	0.00	0.06	0.02
CLASS	0.07	0.04	0.12	0.07
JULES All-band	0.02	0.01	0.05	0.04
GISS II	0.01	0.01	0.05	0.03

$$^a MB = \frac{1}{N} \sum_{i=1}^N (\Delta\alpha_{Model} - \Delta\alpha_{Obs.})$$

S.6. Contribution Analysis: Snow Metamorphosis and Vegetation Structure

An additional set of simulations is executed to discern the relative importance of vegetation structure and temperature in ground masking and snow albedo parameterizations, respectively.

The scheme used for a control is an older MOSES scheme described in Cox et al. (1999) and employed in Betts (2000). MOSES can be classified as a “Type 3” scheme in which albedo is a weighted sum of the snow-free and snow albedo, with weights determined by snow cover (Qu and Hall, 2007). Vegetation structure is not considered, and snow albedo is diagnosed using temperature. We henceforth label and refer to this scheme as “MOSES – Control”.

Myhre and Myhre (2003) adapt this same scheme but do not diagnose snow albedo using temperature to account for snow metamorphosis effects, a scheme we henceforth refer to as “MOSES – No temp.”.

The current JULES All-band scheme (Best, 2009) is based on the older MOSES scheme yet has been updated to include ground-masking effects by vegetation through the introduction of a “radiative fraction” term (f_r) that is based on LAI.

In order to isolate the sensitivity of structure and temperature parameterizations on total albedo, identical snow and vegetation-dependent albedo parameters are applied across all three model versions and may be found in Table S2.

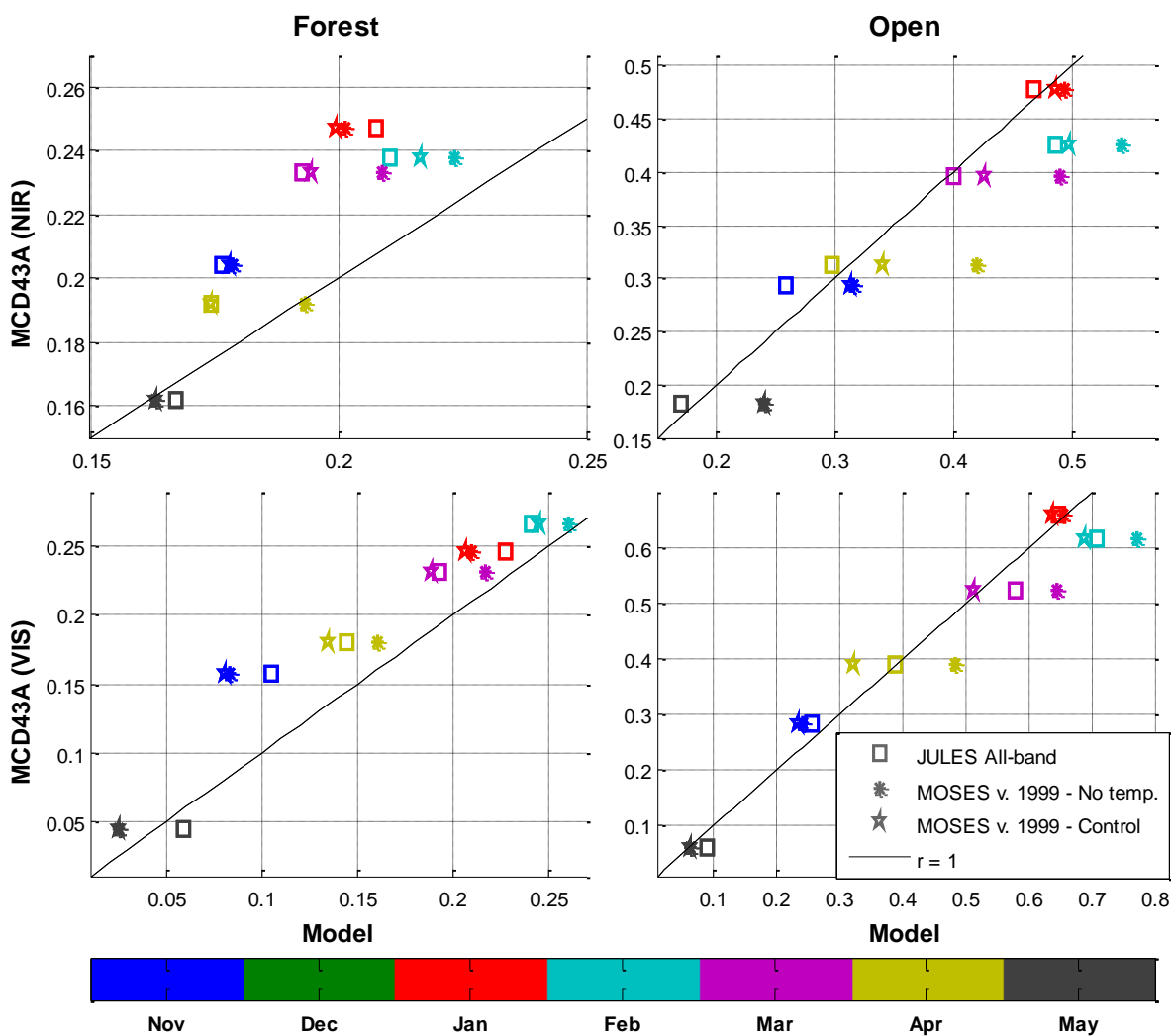


Figure S47. Albedo results for UKMO albedo parameterizations as they have evolved to include snow metamorphosis and vegetation structure effects.

Evident in the regional mean albedo predictions at open areas in Figure S48 (right column) is the improved accuracy when the temperature diagnostic snow albedo parameterization is included. All else being equal, the positive bias (both NIR and VIS) seen in the “No temp.” MOSES scheme is greatly reduced in the “Control” scheme during months with persistent snow cover (Jan. – Mar.). Bias is further reduced – particularly in months without persistent snow cover (Nov., Apr., May.) – when the radiative fraction term is introduced, as in the JULES “All-band” scheme (and MOSES v. ≥ 2.2). The introduction of this term results in a stronger contribution from soil (as opposed to vegetation) to the snow-free albedo term (α_0).

In forests and in particular the NIR band, negative bias is seen in the schemes with temperature diagnostic snow albedo parameterizations (JULES “All-band” and MOSES “Control”) in all months except May. Here, the MOSES “No temp” scheme leads to more accurate predictions. The explanation here is that the parameter for cold deep-snow albedo of forested vegetation (α_s^0) is too low to begin with. The same is true for the VIS band although the bias is less severe.

References

- Aguado, E.: Radiation balances of melting snow covers at an open site in the central Sierra Nevada, California, *Water Resources Research*, 21, 1649-1654, 1985.
- Aoki, T., Hachikubo, A., and Hori, M.: Effects of snow physical parameters on shortwave broadband albedos, *Journal of Geophysical Research: Atmospheres*, 108, 4616, 2003.
- Asner, G. P., Wessman, C. A., Schimel, D. S., and Archer, S.: Variability in leaf and litter optical properties: implications for BRDF model inversions using AVHRR, MODIS, and MISR, *Remote Sensing of Environment*, 63, 243-257, 1998.
- Bartlett, P. A., MacKay, M. D., and Verseghy, D. L.: Modified snow algorithms in the Canadian land surface scheme: Model runs and sensitivity analysis at three boreal forest stands, *Atmosphere-Ocean*, 44, 207-222, 2006.
- Best, M.: JULES Technical Documentation, Met Office, Joint Centre for Hydro-Meteorological Research, Wallingford, U.K., 2009.
- Best, M. J., Pryor, M., Clark, D. B., Rooney, G. G., Essery, R. L. H., Ménard, C. B., Edwards, J. M., Hendry, M. A., Porson, A., Gedney, N., Mercado, L. M., Sitch, S., Blyth, E., Boucher, O., Cox, P. M., Grimmond, C. S. B., and Harding, R. J.: The Joint UK Land Environment Simulator (JULES), model description – Part 1: Energy and water fluxes, *Geosci. Model Dev.*, 4, 677-699, 2011.
- Betts, A. K. and Ball, J. H.: Albedo over the boreal forest, *Journal of Geophysical Research*, 102, 28901-28909, 1997.
- Betts, R. A.: Offset of the potential carbon sink from boreal forestation by decreases in surface albedo, *Nature*, 408, 187-190, 2000.
- Bright, R. M., Antón-Fernández, C., Astrup, R., and Strømman, A. H.: Empirical models of albedo transitions in managed boreal forests: Analysis of performance and transportability, *Canadian Journal of Forest Research*, DOI: 10.1139/cjfr-2014-0132 2014.
- Bright, R. M., Astrup, R., and Strømman, A. H.: Empirical models of monthly and annual albedo in managed boreal forests of interior Norway, *Climatic Change* 120, 183-196, 2013.
- Broch, B. W., Willis, I. C., and Sharp, M. J.: Measurement and parameterization of albedo variations at Haut Glacier d'Arolla, Switzerland, *Journal of Glaciology*, 2, 374-394, 2000.
- Brun, E.: Investigation on wet-snow metamorphism in respect of liquid-water content, *Annals of Glaciology*, 13, 22-26, 1989.

- Cox, P. M., Betts, R. A., Bunton, C. B., Essery, R. L. H., Rowntree, P. R., and Smith, J.: The impact of new land surface physics on the GCM simulation of climate and climate sensitivity, *Climate Dynamics*, 15, 183-203, 1999.
- Dickinson, R. E.: Land surface processes and climate-surface albedos and energy balance, *Advances in Geophysics*, 25, 305-353, 1983.
- Dickinson, R. E., Henderson-Sellers, A., and Kennedy, P. J.: Biosphere-Atmosphere Transfer Scheme (BATS) version 1e as coupled to the NCAR Community Climate Model. NCAR Technical Note 387., National Center for Atmospheric Research (NCAR), Boulder, Colorado, USA, 251 pp., 1993.
- Dirmhirn, I. and Eaton, F. D.: Some characteristics of the albedo of snow, *Journal of Applied Meteorology*, 14, 375-379, 1975.
- Dorman, J. L. and Sellers, P.: A global climatology of albedo, roughness length, and stomatal resistance for atmospheric general circulation models as represented by the simple biosphere model (SiB), *Journal of Applied Meteorology*, 28, 833-855, 1989.
- Essery, R., Best, M., and Cox, P.: MOSES 2.2 Technical documentation. Hadley Centre Technical Note 30, U.K. Met Office Hadley Centre, Exeter, U. K., 1-31 pp., 2001.
- Essery, R., Morin, S., Lejeune, Y., and B Ménard, C.: A comparison of 1701 snow models using observations from an alpine site, *Advances in Water Resources*, 55, 131-148, 2013.
- Gao, F., Schaaf, C. B., Strahler, A. H., Roesch, A., Lucht, W., and Dickinson, R. E.: MODIS bidirectional reflectance distribution function and albedo Climate Modeling Grid products and the variability of albedo for major global vegetation types, *Journal of Geophysical Research*, 110, 1-13, 2005.
- Goudriaan, J.: The bare bones of leaf angle distribution in radiation models for canopy photosynthesis and energy exchange, *Agricultural and Forest Meteorology*, 43, 155-169, 1988.
- Granhus, A., Hylen, G., and Nilsen, J.-E. Ø.: Statistics of forest conditions and resources in Norway, Norwegian Forest and Landscape Institute, Ås, 2012.
- Hansen, J., Russell, G., Rind, D., Stone, P., Lacis, A., Lebedeeff, S., Ruedy, R., and Travis, L.: Efficient three-dimensional global models for climate studies: Models I and II., *Monthly Weather Review*, 111, 609-662, 1983.
- Hedstrom, N. R. and Pomeroy, J. W.: Measurements and modelling of snow interception in the boreal forest, *Hydrological Processes*, 12, 1611-1625, 1998.
- Kuusinen, N., Kolari, P., Levula, J., Porcar-Castell, A., Stenberg, P., and Berninger, F.: Seasonal variation in boreal pine forest albedo and effects of canopy snow on forest reflectance, *Agricultural and Forest Meteorology*, 164, 53-60, 2012.
- Lawrence, P. J. and Chase, T. N.: Representing a new MODIS consistent land surface in the Community Land Model (CLM 3.0), *Journal of Geophysical Research: Biogeosciences*, 112, G01023, 2007.
- Meløysund, V., Leira, B., Høiseth, K. V., and Lisø, K. R.: Predicting snow density using meteorological data, *Meteorological Applications*, 14, 413-423, 2007.
- Miller, D.: Snow in trees -- where did it go?, Proceedings of the 30th annual meeting of the Western Snow Conference, 30, 21-29, 1962.
- Myhre, G. and Myhre, A.: Uncertainties in Radiative Forcing due to Surface Albedo Changes Cause by Land-Use Changes, *Journal of Climate*, 16, 1511-1524, 2003.
- Mölders, N., Luijting, H., and Sassen, K.: Use of atmospheric radiation measurement program data from Barrow, Alaska, for evaluation and development of snow-albedo parameterizations, *Meteorol Atmos Phys*, 99, 199-219, 2008.
- Nakai, Y., Sakamoto, T., Terajima, T., Kitahara, H., and Saito, T.: Snow interception by forest canopies: weighing a conifer tree, meteorological observation and analysis by the Penman-Monteith formula, IAHS Publications, 223, 227-236, 1994.
- Niu, G.-Y. and Yang, Z.-L.: An observation-based formulation of snow cover fraction and its evaluation over large North American river basins, *Journal of Geophysical Research: Atmospheres*, 112, D21101, 2007.
- Norwegian Meteorological Institute: eKlima - Daily Historical Meteorology. Norwegian Meteorological Institute. Accessed Sept. 15, 2013 at:

http://sharki.oslo.dnmi.no/portal/page?_pageid=73,39035,73_39049&_dad=portal&_schema=PORTAL

2013a.

Norwegian Meteorological Institute: eKlima - Monthly Historical Meteorology. Norwegian Meteorological Institute. Accessed Jan 31, 2013 at:

http://sharki.oslo.dnmi.no/portal/page?_pageid=73,39035,73_39049&_dad=portal&_schema=PORTAL

2013b.

Oleson, K., Dai, Y., Bonan, G. B., Bosilovich, M. G., Dickinson, R. E., Dirmeyer, P. A., Hoffman, F., Houser, P., Levis, S., Niu, G.-Y., Thornton, P. E., Vertenstein, M., Yang, Z.-L., and Zeng, X.: Technical description of the Community Land Model (CLM). NCAR Technical Note 461, National Center for Atmospheric Research (NCAR), Boulder, Colorado, USA, 174 pp., 2004.

Oleson, K., Lawrence, D. M., Bonan, G. B., Flanner, M. G., Kluzek, E., Lawrence, P. J., Levis, S., Swenson, S. C., Thornton, P. E., Dai, A., Decker, M., Dickinson, R. E., Feddema, J. J., Heald, C. L., Hoffman, F., Lamarque, J. F., Mahowald, N., Niu, G.-Y., Qian, T., Randerson, J., Running, S. W., Sakaguchi, A. S., Stöckli, R., Wang, A., Yang, Z.-L., Zeng, X., and Zeng, X.: Technical description of version 4.0 of the Community Land Model (CLM), National Center for Atmospheric Research, Climate and Global Dynamics Division, Boulder, CO, USA, 266 pp., 2010.

Otto, J., Raddatz, T., and Claussen, M.: Strength of forest-albedo feedback in mid-Holocene climate simulations, *Clim. Past*, 7, 1027-1039, 2011.

Pedersen, C. and Winther, J.-G.: Intercomparison and validation of snow albedo parameterization schemes in climate models, *Climate Dynamics*, 25, 351-362, 2005.

Peel, M. C., Finlayson, B. L., and McMahon, T. A.: Updated world map of the Köppen-Geiger climate classification, *Hydrology and Earth System Sciences*, 11, 1633-1644, 2007.

Pirazzini, R.: Challenges in snow and ice albedo parameterizations, *Geophysica* 45, 41-62, 2009.

Qu, X. and Hall, A.: What Controls the Strength of Snow-Albedo Feedback?, *Journal of Climate*, 20, 3971-3981, 2007.

Reick, C. H., Gayler, V., Raddatz, T., and Schnur, R.: JSBACH - The new land component of ECHAM, Max Planck Institute for Meteorology, Hamburg, Germany, 1-167 pp., 2012.

Robinson, D. A. and Kukla, G.: Albedo of a disappearing snow cover, *Journal of Applied Meteorology*, 23, 1626-1634, 1984.

Roesch, A., Wild, M., Gilgen, H., and Ohmura, A.: A new snow cover fraction parametrization for the ECHAM4 GCM, *Climate Dynamics*, 17, 933-946, 2001.

Rutter, N., Essery, R., Pomeroy, J., Altimir, N., Andreadis, K., Baker, I., Barr, A., Bartlett, P., Boone, A., Deng, H., Douville, H., Dutra, E., Elder, K., Ellis, C., Feng, X., Gelfan, A., Goodbody, A., Gusev, Y., Gustafsson, D., Hellström, R., Hirabayashi, Y., Hirota, T., Jonas, T., Koren, V., Kuragina, A., Lettenmaier, D., Li, W.-P., Luce, C., Martin, E., Nasonova, O., Pumpanen, J., Pyles, R. D., Samuelsson, P., Sandells, M., Schädler, G., Shmakin, A., Smirnova, T. G., Stähli, M., Stöckli, R., Strasser, U., Su, H., Suzuki, K., Takata, K., Tanaka, K., Thompson, E., Vesala, T., Viterbo, P., Wiltshire, A., Xia, K., Xue, Y., and Yamazaki, T.: Evaluation of forest snow processes models (SnowMIP2), *Journal of Geophysical Research: Atmospheres*, 114, D06111, 2009.

Schmidt, G. A., Ruedy, R., Hansen, J. E., Aleinov, I., Bell, N., Bauer, M., Bauer, S., Cairns, B., Canuto, V., Cheng, Y., Del Genio, A., Faluvegi, G., Friend, A. D., Hall, T. M., Hu, Y., Kelley, M., Kiang, N. Y., Koch, D., Lacis, A. A., Lerner, J., Lo, K. K., Miller, R. L., Nazarenko, L., Oinas, V., Perlitz, J., Perlitz, J., Rind, D., Romanou, A., Russell, G. L., Sato, M., Shindell, D. T., Stone, P. H., Sun, S., Tausnev, N., Thresher, D., and Yao, M.-S.: Present-Day Atmospheric Simulations Using GISS ModelE: Comparison to In Situ, Satellite, and Reanalysis Data, *Journal of Climate*, 19, 153-192, 2006.

Schmidt, R. A. and Gluns, D. R.: Snowfall interception on branches of three conifer species, *Canadian Journal of Forest Research*, 21, 1262-1269, 1991.

- Sellers, P. J.: Canopy reflectance, photosynthesis, and transpiration, International Journal of Remote Sensing, 6, 1335-1372, 1985.
- Verseghy, D. L.: CLASS - The Canadian land surface scheme (version 3.4) - Technical documentation (version 1.1), Environment Canada, Quebec, Canada, 1-183 pp., 2009.
- Verseghy, D. L., McFarlane, N. A., and Lazare, M.: CLASS - A Canadian land surface scheme for GCMs. II. Vegetation model and coupled runs, International Journal of Climatology, 13, 347-370, 1993.
- Wang, Z. and Zeng, X.: Evaluation of Snow Albedo in Land Models for Weather and Climate Studies, Journal of Applied Meteorology and Climatology, 49, 363-380, 2009.
- Wiscombe, W. J. and Warren, S. G.: A model for the spectral albedo of snow. I. Pure Snow, Journal of Atmospheric Science, 37, 2712-2733, 1980.
- Yamazaki, T., Fukabori, K., and Kondo, J.: Albedo of a forest with crown snow, Journal of the Japanese Society of Snow and Ice, 58, 11-18, 1996.
- Yang, Z.-L., Dickinson, R. E., Robock, A., and Vinnikov, K. Y.: Validation of the Snow Submodel of the Biosphere–Atmosphere Transfer Scheme with Russian Snow Cover and Meteorological Observational Data, Journal of Climate, 10, 353-373, 1997.
- Zeng, X., Shaikh, M., Dai, Y., Dickinson, R. E., and Myneni, R.: Coupling of the Common Land Model to the NCAR Community Climate Model, Journal of Climate, 15, 1832-1854, 2002.